The role of HuR in the crosstalk between tumor cells and macrophages

Dissertation

zur Erlangung des Doktorgrades

der Naturwissenschaften

vorgelegt beim Fachbereich 14

der Johann Wolfgang Goethe-Universität

in Frankfurt am Main

von

Thilo Brauß

aus Karlsruhe

Frankfurt am Main 2019

(D 30)

vom Fachbereich 14 der

Johann Wolfgang Goethe-Universität als Dissertation angenommen.

Dekan: Prof. Dr. Clemens Glaubitz

Gutachter:

Datum der Disputation:

Index

List of figures

List of tables

Abbreviations

AP1	activator protein 1
ARE	adenylate/uridylate (AU)- and U-rich element
AUBP	ARE-binding protein
AUF1	AU-rich element RNA-binding protein 1
Bcl-xL	B-cell lymphoma extra large
C/EBP	CCAAT enhancer binding protein
CAF	cancer associated fibroblast
CBA	cytometric bead array
CCL	C-C chemokine ligand
CCR	C-C chemokine receptor
CD	cluster of differentiation
ChIP	chromatin immunoprecipitation
COX2	cyclooxygenase 2
CREB	cAMP response element-binding protein
ctrl	control
DNA	desoxyribonucleic acid
e.g.	for example
ECM	extracellular matrix
ELAVL1	embryonic lethal abnormal vision-like 1
ER	estrogen receptor
et al.	and others
FACS	fluorescence-activated cell sorting
GM-CSF	granulocyte-macrophage colony-stimulating factor
H3	histone 3
HGNC	Human Genome Organisation (HUGO) Gene Nomenclature Committee
HIF	hypoxia-inducible factor
HuR	human antigen R
IFN	interferon
IFNAR	interferon-α/β receptor

IGFBP4	insulin-like growth factor-binding protein 4
IgG	immunoglobulin G
IL	interleukin
IRF	interferon regulatory factor
ISGF3	IFN-stimulated gene factor 3 complex
ISRE	interferon-stimulated response element
JNK	c-Jun N-terminal kinase
kd	knockdown
kDa	kilodalton
KLF13	krueppel-like factor 13
KSRP	KH-type splicing regulatory protein
LPS	lipopolysaccharides
MAPK	mitogen-activated protein kinase
MHCII	class II major histocompatibility complex
MMP	matrix metalloproteinase
MO	monocyte
mRNA	messenger RNA
MSR1	macrophage scavenger receptor 1
MΦ	macrophage
n	statistical sample size
NF-κB	nuclear factor kappa-light-chain-enhancer of activated B cells
PCR	polymerase chain reaction
PDGF	platelet-derived growth factor
PIM	protease inhibitor mix
PMSF	phenylmethylsulfonyl fluoride
PPARγ	peroxisome proliferator-activated receptor gamma
prom	promoter
qPCR	quantitative PCR
RANTES	regulated upon activation, normal T-cell expressed and secreted (=CCL5)
RBP	RNA binding protein

RNA	ribonucleic acid
RRM	RNA recognition motif
SEM	standard error of the mean
sh	small hairpin
Stat	signal transducer and activator of transcription
SV40	simian virus 40
TAM	tumor-associated macrophage
TGFβ	transforming growth factor beta
TNFα	tumor necrosis factor alpha
TTP	tristetraprolin
UTR	untranslated region
VEGF	vascular endothelial growth factor

1 Zusammenfassung

Krebs ist und wird voraussichtlich auch in näherer Zukunft eine der häufigsten Todesursachen weltweit bleiben. Trotz vielversprechenden Fortschritten in Therapeutik und Diagnostik bedarf es noch weiterer Forschung, um die vielfältigen molekularen Mechanismen zu entschlüsseln, welche dem Verlauf von malignen Tumorerkrankungen bestimmen und zu beeinflussen vermögen. Das RNA-Bindeprotein *Human antigen R* (HuR) reguliert Genexpression auf posttranskriptioneller Ebene, indem es durch Bindung an Ziel mRNAs Einfluss auf deren Abbau, Lokalisation oder Translationseffizienz nimmt. Darüber hinaus zeigte sich in den letzten Jahren, dass HuR diese Prozesse auch indirekt durch Interaktion mit regulatorischen RNAs beeinflusst. In Krebszellen lässt sich häufig eine erhöhte Aktivität von HuR beobachten, welche in Verbindung mit verschiedenen tumorigenen Prozessen gebracht wird. Unter anderem trägt HuR zur Deregulation des Zellzyklus bei, indem es die Expression der Cycline A2, B1, D1 und E1 erhöht. Weiterhin unterstützt HuR das Tumorwachstum durch Regulation von proangiogenen Faktoren wie VEGF, IL8 und COX2. Da HuR generell eine prominente Rolle bei der Regulation von Immunantworten, sowohl in Immunzellen selbst als auch in solidem Gewebe einnimmt, wurde HuR in der Vergangenheit häufig auch mit der Ausbildung des inflammatorischen Tumormikromilieus in Verbindung gebracht, jedoch ist die Datenlage in dieser Hinsicht bis heute uneindeutig. Obwohl eine Großzahl an Zytokinen und inflammatorischen Faktoren prinzipiell als HuR Zielgene beschrieben sind, gibt es nur für die wenigsten dieser Proteine entsprechende Untersuchungen in Tumorzellen.

Ziel dieser Arbeit war es, den Einfluss von HuR in Tumoren auf die Rekrutierung von Makrophagen zu evaluieren. Hierfür bot sich als in vitro Modell die Brustkrebszelllinie MCF-7 an, da diese unter entsprechenden Kultivierungsbedingungen dreidimensionale Sphäroide bildet. Solch ein Sphäroidmodell bietet sich als Kompromiss zwischen der klassischen zweidimensionalen Zellkultur an, welche zwar höchst artifiziell, jedoch leicht zu handhaben und zu kontrollieren ist, und den physiologischeren, aber gleichzeitig experimentell unzugänglicheren und speziesfremden Tiermodellen. Mittels lentiviraler Transduktion wurde ein *small hairpin* RNA (shRNA) vermittelter stabiler

Knockdown von HuR in MCF-7 erzielt, welcher zu vermindertem Zellwachstum führte, jedoch keinen weiteren Einfluss auf die Bildung von Sphäroiden hatte. Um die initiale Suche nach HuR-regulierten, potenziell relevanten Faktoren möglichst breit und unvoreingenommen zu halten, wurde die Expression von 174 Zytokinen in Wildtyp- und HuR-*knockdown* Sphäroiden mittels eines Protein Arrays untersucht. Überraschenderweise zeigte der Großteil der veränderten Proteins einen negativen Zusammenhang mit HuR, welches eigentlich eher als positiv regulierendes Protein beschrieben ist. Bemerkenswerterweise befand sich unter den mit am stärksten regulierten Faktoren das Chemokin CCL5 (auch RANTES genannt), welches einerseits als einer der beiden zentralen Faktoren für die Makrophageninfiltration in Brustkrebs gilt, andererseits bisher noch nicht in Verbindung mit HuR gebracht wurde.

Im Folgenden untersuchte ich zuerst den mechanistischen Hintergrund dieser Regulation. Da diese sich auch in adhärenten Zellrasen zeigte, wechselte ich für die entsprechenden Experimente zu zweidimensionaler Zellkultur. Eine negative regulatorische Funktion von HuR wird meist in Verbindung mit verminderter Translation von Zielfaktoren gebracht. Da die mRNA Level von CCL5 dem Effekt auf Proteinebene entsprachen, konnten entsprechende Mechanismen als Grund für die veränderten CCL5 Level ausgeschlossen werden. Desweiteren blieb die mRNA Stabilität ungeachtet der HuR Level konstant; dabei zeigte sich zudem, dass mRNA Abbau generell keinen relevanten Einfluss auf die Expression von CCL5 in MCF-7 hatte. Da diese Ergebnisse auf eine transkriptionelle Regulation hindeuteten, untersuchte ich im Folgenden den Einfluss von HuR auf die Promoteraktivität von CCL5. Hierfür isolierte ich zunächst die CCL5-Promoterregion aus genomischer DNA von MCF-7 Zellen und inserierte diese dann in einen zuvor promoterlosen Luciferase-Expressionsvektor. In den folgenden Reporteranalysen zeigte sich, dass HuR tatsächlich einen negativen Einfluss auf die Promoteraktivität von CCL5 ausübt. Durch sukzessive Verkürzung ließ sich der entscheidende DNA-Bereich auf die letzten 140 Nukleotide vor dem Transkriptionsstartpunkt eingrenzen. Dieser Bereich enthält vier prominente und sehr gut charakterisierte regulatorische Abschnitte: zwei benachbarte NF-κB Bindestellen sowie je ein *Interferon-stimulated Response Element* (ISRE) und ein C/EBPβ Erkennungsmotiv. Während das C/EBP Element keine funktionelle Relevanz in den Reporteranalysen hatte, reduzierte sich durch Deletion sowohl der ISRE als auch der NF-κB Elemente die Promoteraktivität

um mehr als 50%, allerdings nur im ISRE-Deletionskonstrukt unter Nivellierung des HuR-abhängigen Unterschiedes. Somit ließ sich der Einfluss von HuR auf die CCL5 Promoteraktivität vollständig und ausschließlich auf das ISRE zurückführen. Im Gegensatz zu dem in Tumorzellen häufig basal überaktiven NF-κB Signalweg sind die kanonischen, ISRE-assoziierten Typ I Interferon Signalkaskaden und ihre vermittelnden Transkriptionsfaktoren, die sogenannten *Interferon Regulatory Factors* (IRFs) nicht konstitutiv überaktiviert. Eine Sonderstellung nehmen dabei die Faktoren IRF1 und IRF2 ein, da sie, für Proteine abseits der Stimulus-getriebenen ISRE-Interferon Achse, auch als konstitutive Transkriptionsfaktoren beschrieben sind, wobei IRF2 in diesem Kontext als IRF1-Antagonist und somit Transkriptionsrepressor fungiert. Überraschenderweise ließ sich mittels Chromatin Immunopräzipitation eine Assoziation von IRF1 mit dem CCL5 Promoter nur in Wildtyp-, jedoch nicht in HuR-*knockdown* Zellen nachweisen. Im Gegensatz dazu ergaben mRNA Expressionsanalysen der Tumor-relevanten IRFs, dass die CCL5 Induktion in HuR-depletierten Zellen mit einer allgemeinen, jedoch niedrigschwelligen Erhöhung von Typ I Interferon-assoziierten Signalen einhergeht. Interessanterweise korrelierte Interferon β zwar mit CCL5 auf mRNA Ebene, jedoch hatte eine Blockade des Interferon-α/β Rezeptors in HuR-depletierten Zellen keinen akuten Effekt auf CCL5. Umgekehrt zeigte sich auch keine erhöhten CCL5 Level in Wildtypzellen unter Kokultur mit HuR-*knockdown* Zellen, wie es bei parakriner Induktion durch Interferon β zu erwarten wäre. Ebenso konnte alternatives ISRE Signaling durch einen Komplex aus unphosphoryliertem Stat1 und IRF9, wie es *in vitro* unter länger anhaltender Niedriglevel Exposition mit Interferon β beobachtet wurde, ausgeschlossen werden. Um sicher zu stellen, dass diese Erhöhung kein sequenzabhängiges *off-target* Artefakt ist, wie es in der Vergangenheit für einzelne *small hairpin* RNAs (shRNAs) beobachtet wurde, wurde eine entsprechende Aktivierung von IRF3 und damit des IRF3/IRF7 Aktivierungsweges untersucht und ausgeschlossen. Zusätzlich konnte durch Tests unterschiedlicher shRNA Sequenzen sowie Zellsysteme demonstriert werden, dass die CCL5 Aktivierung tatsächlich ein spezifischer und in einer größeren Bandbreite an Krebszelllinien unterschiedlicher Herkunft, darunter Brust- und Lungenkarzinom, Glioblastom- sowie Melanom- Zelllinien, reproduzierbarer Effekt von HuR-Defizienz ist.

Da CCL5 als eines der zentralen Chemokine bei der Rekrutierung von Monozyten/Makrophagen in Tumore beschrieben ist, stellte sich die Frage, ob HuR

mit diesem Vorgang in Verbindung zu bringen ist. Brusttumore weisen oft eine hohe Zahl von Tumor-assoziierten Makrophagen auf, welche von eingewanderten Blutmonozyten abstammen. Ein Einfluss von HuR auf diesen Vorgang *in vitro* konnte mittels einer Kokultur von Sphäroiden mit zuvor frisch aus Humanblut isolierten Primärmonozyten nachgewiesen werden. Hierbei wiesen HuR-*knockdown* Sphäroide trotz ihres geringeren Durchmessers eine erhöhte Anzahl von Monozyten/Makrophagen auf. Da sich in diesen Zellen weder Proliferation noch relevante Apoptose zeigte, ließ sich die erhöhte Anzahl auf verstärkte Einwanderung in das Sphäroid zurückführen. Hierbei erwies sich der direkte Zellkontakt zwischen Monozyten und Tumorzellen als erforderlich, da Monozyten keine unterschiedliche Chemotaxis gegenüber entsprechenden Sphäroidüberständen zeigten. Dass die erhöhte Infiltration in HuR-defizienten Sphäroiden tatsächlich auf CCL5 zurückzuführen ist, konnte in Kokulturexperimenten durch Inhibierung von CCL5 gezeigt werden. Unterstützend wurde ein Zusammenhang zwischen HuR, CCL5 und Tumor assoziierten Makrophagen *in silico* unter Zuhilfenahme des TCGA Datensets für Estrogenrezeptor-positive Brusttumore untersucht. Im Einklang mit meinen Ergebnissen zeigte sich eine negative Korrelation zwischen HuR und CCL5. Außerdem ließ sich ein negativer Zusammenhang zwischen HuR und einer Makrophagensignatur feststellen, während CCL5 wie erwartet mit dieser Signatur positiv korrelierte.

Zusammenfassend zeigte sich in dieser Arbeit, dass HuR eine Rolle bei der zellulären Zusammensetzung des inflammatorischen Tumor-Mikromilieus spielt. Der Verlust von HuR in Tumorzellen führte zu einer erhöhten Expression des Chemokins CCL5. Dies ließ sich in Brust- und Lungenkarzinom-, Glioblastom- sowie Melanom- Zelllinien beobachten. In Brustkrebszellen zeigte sich, dass diese Regulation auf verstärkte Transkription, vermittelt durch ein ISRE innerhalb des CCL5 Promoters, zurückzuführen ist. Funktionell konnte die erhöhte CCL5 Produktion in HuR-defizienten Tumorsphäroiden in Verbindung mit verstärkter Infiltration von Monozyten/Makrophagen gebracht werden. Unterstützend zeigte sich auch bei einer *in silico* Analyse von Estrogenrezeptor-positiven Brusttumoren eine negative Korrelation zwischen HuR und CCL5, was mit einer entsprechend veränderten Makrophagensignatur einherging. Im Hinblick auf derzeit diskutierte Ansätze, das Wachstum von Tumoren mittels HuR Blockade zu inhibieren, sind

meine Ergebnisse potenziell von therapeutischer Relevanz. Basierend auf meiner Arbeit sollte dabei in zukünftigen Studien näher untersucht werden, wie sich Inhibierung von HuR in Tumoren auf die Zusammensetzung und Funktion des Tumormikromilieus auswirkt und daraus resultierende Effekte auf das Tumorwachstum in Relation zu der allgemein wachstumsfördernden Rolle von HuR in Tumorzellen gesetzt werden.

2 Introduction

2.1 Cancer

Cancer is considered to be one of the overall most life-threatening diseases, in matters of severity as well as incidence. Moreover, it can develop spontaneously without any prior indications and at any age. Despite the huge efforts and promising progress in cancer research and medicine, it remains one of the three most common global causes of death. The reason why cancer still resists so persistently any general cure, is rooted in its heterogeneity and highly adaptive nature. Thus, it is a necessity to identify and study the underlying biological principles of tumor development. The obsolete perception that an alien tumor entity resides as a separated foreign matter inside the host was already dismissed a long time ago. When being formed, malignant tumors are now considered an integrated part of the organism which we can only understand if we acknowledge the dynamic interplay between cancer and host.

2.1.1 The paradigm(s) of carcinogenesis

Cancer appears as an aggressive expansion of abnormal cells invading and compromising surrounding tissues and spreading into distant parts of the body. While cells showing genetic abnormalities are surprisingly numerous in a healthy organism, cancer is a relatively rare phenomenon due to the fact that, if this mutation gets apparent, the cell usually gets apoptotic or is recognized and eliminated by the host immune system [1]. Additionally, several protective mechanisms limit the reproductive potential of a cell, allow for DNA repair, and prevent uncontrolled spreading. Cancer only emerges if such malfunctional cells undergo a process called malignant transformation, where they acquire all the necessary properties to form a tumor [2].

Obviously, this geno- and phenotypical reprogramming does not happen intentionally, but rather occurs as the consequence of a selection process, pointing to the fact that cancer emerges in a not predetermined manner and only if cells acquire certain malignant properties. However, it is hard to understand why and how normal tissue cells may transform into such perfectly adapted and aggressive cancer cells just by random mutation events. Aggravating the situation, this transformation has to

be accomplished within the organism's lifespan and, above all, is happening in spite of endogenous control mechanisms as well as under the survey of an immune system, which should be evolutionary primed to prevent this process [3].

In 1976, Nowell was the first to acknowledge the importance of evolutionary principles for this process and postulated a model of several consecutive rounds of clonal selection, where the cells may gain these malignant properties in a distinct order [4]. This general framework has been developed over the last decades by incorporating new theories, evolutionary processes, and findings further substantiating the general concept [5, 6]. In 2000, Hanahan and Weinberg introduced the meanwhile widely established term 'hallmarks of cancer' to describe and categorize such key traits every malignant tumor inevitably acquires [7]. The 2011 updated version defines 10 such key characteristics [8]. This summary gives a comprehensive overview of the current knowledge and provides a coherent model compellingly showing that, despite the random nature of genetic mutations and no matter from which tissue the cancer originates, all tumors eventually share some defined and mandatory characteristics.

2.1.2 The tumor microenvironment

The hallmarks of cancer include several aspects that are mediated by, or at least vastly dependent on, cells of the tumor stroma [9]. However, for a long time the biology of a tumor was mainly reduced to cancer cell functions, while the presence of stromal cells within the tumor was carelessly neglected. This view changed dramatically over the last two decades, as increasing evidence substantiated the concept that cancer cells actively shape their microenvironment by the specific attraction and corruption of cells of the stroma which then exert tumor supporting functions [10]. At first sight, this trait may appear as a sinister force to brainwash other cells, however, a closer look reveals that the cancer cells merely take advantage of existing molecular mechanisms originally designed for other processes, such as embryonic development, wound healing, or resolution of inflammation.

It is important to note that the tumor promoting conditions provided by the tumor microenvironment do not exclusively result from processes brought about by specific malignant traits, yet commonly are concomitant effects of general tumor growth, though they possess tumor promoting traits. For example, the aberrant tumor vasculature leads to local hypoxia and apoptosis which both can contribute to

immunotolerance of tumor associated macrophages (TAMs) [11].

The microenvironment of solid tumors is surprisingly uneven in matters of its cellular composition as well as the environmental conditions. It is furthermore subject to dynamic changes resulting from permanent remodeling of extracellular matrix (ECM) and vascular structures, cell migration, and tumor growth. Additionally, cancer cells and the local tumor microenvironment mutually shape each other in a continuous interplay. As a consequence of this diversity, even a monoclonal cancer cell population may give rise to a heterogeneous tumor that exhibits a broad spectrum of cancer cell phenotypes with a high spatial and temporal plasticity. Moreover, some regions within a tumor may provide local environmental niches leading to defined cancer cell subpopulations with exclusive characteristics such as stemness or metastatic potential.

The most apparent component of the tumor stroma are blood vessels formed by endothelial cells. Every tissue needs constant supply of oxygen and nutrients and the possibility to discharge carbon dioxide and metabolic waste. Hence, macroscopic tumor growth requires the ability to permanently stimulate angiogenesis. It has been noted though that the resulting vascular structure is chaotically organized and rather instable, which leads to a heterogeneous tumor microenvironment with hypoxic regions [12]. Moreover, tumor associated vessels were observed to lack a proper coverage by pericytes, which may facilitate tumor cell intravasation and metastasis [13].

ECM remodeling is an important step for malignant transformation and progression as it is the prerequisite for the majority of cancer hallmarks including the formation of a tumor stroma [14]. This process is mainly driven by cancer associated fibroblasts (CAFs), which are one of the most abundant stromal cell populations in most solid tumors. Unlike the inactive fibroblasts in healthy tissue, CAFs, activated by transforming growth factor beta (TGFβ) and matrix degradation, rather resemble the activated wound healing fibroblasts. Their activation is highly dependent on TGFβ secretion by the tumor cells, but once activated they also secrete TGFβ by themselves, thereby supporting cancer invasiveness [15]. Upon activation, CAFs account for the bulk of matrix metalloproteinases (MMPs) and matrix components and are the central mediators of further ECM remodeling. Moreover, they secrete vascular endothelial growth factor (VEGF) and platelet-derived growth factor (PDGF)

and contribute substantially to angiogenesis and metastasis [16].

In the context of the interaction between tumors and their microenvironment, it is important to note that solid tumors are often characterized by a massive and steady influx of leukocytes, most notably macrophages, neutrophils, and T-cells, which create an inflammatory microenvironment.

2.2 Inflammation

Acute inflammation is a transient and local condition in response to pathogens or tissue damage which is mainly carried out by the innate immune system. The inflammatory process starts when resident tissue leukocytes recognize damage- or pathogen-associated molecular patterns and release inflammatory mediators. Consequently, circulating leukocytes, particularly neutrophils, infiltrate into the tissue where they attack pathogens, clean up debris, and secrete further inflammatory mediators leading to vasodilation and more immune cell recruitment. When the damaging stimulus is eliminated, the inflammation resolves. Macrophages play a key role in this resolution phase during which they stimulate cell proliferation, ECM remodeling, and neovascularization in order to restore tissue integrity. However, if the damage stimulus persists or the resolution process is disturbed, the inflammation may turn chronic.

2.2.1 Inflammation and cancer

An evident link between inflammation and cancer appears in the course of several chronic inflammatory diseases which provoke an elevated cancer risk [17]. For example, *Helicobacter pylori* infection is the primary cause for gastric cancer. This pathogen is estimated to reside in over 50% of the world's population, usually causing a local inflammation without any symptoms [18]. Another example is the risk for colorectal cancer, which is 10 fold increased in patients with chronic ulcerating colitis or Crohn's disease [17]. Obesity-induced inflammation has also been associated with cancer progression for several tumor sites. The predominant mechanisms that links chronic inflammation to cancer onset is suggested to be DNA damage as a consequence of reactive oxygen/nitrogen species produced by inflammatory leukocytes [20]

However, when looking from the other side, the link becomes even more striking. Even tumors that do not arise from an inflammatory milieu actively recruit immune

cells eventually leading to an inflammatory microenvironment. Persistent inflammation caused by continuous tissue disruption, presence of inflammatory mediators, and immune cell recruitment is a central characteristic of the tumor microenvironment and consequently appears as one of the hallmarks of cancer [8]. In this light, Dvorak already 30 years ago described tumors as ‘wounds that do not heal’ [21], which has become a popular phrase and reference in the last decade. Indeed, the similarities between the inflammatory processes in tumors and wound healing are striking. However, tumors maintain several processes that in wound healing are usually strictly limited in time, e.g. sustained VEGF signaling or fibroblast activation as already described in the last section.

2.2.2 Macrophages

Macrophages (MΦs) derive from myeloid progenitor cells. As a part of the innate immune response, they phagocytose pathogens and stimulate inflammatory responses. Furthermore, they present phagocytosed antigens via the class II major histocompatibility complex (MHCII), thereby connecting the innate to the adaptive arm of the immune system. Additionally, they contribute to the resolution of inflammatory responses and stimulate the repair of damaged tissue in order to restore tissue homeostasis [22]. These diverse functions are dependent on distinct activation stimuli. Two opposing polarization states can be defined, mirroring the dichotomy of type I and type II immune responses.

Classically activated M1 MΦs secrete proinflammatory cytokines like interleukin 1 beta (IL1β), tumor necrosis factor alpha (TNFα), IL6, and IL12, promote antipathogenic T-cell (Th1) responses, and produce reactive oxygen species [23]. They eliminate microorganisms and neoplastic cells, display a high antigen presentation capacity and are able to inhibit the proliferation of surrounding cells. M1 polarization is induced by interferon gamma (IFNγ), alone or in combination with proinflammatory cytokines like TNFα and granulocyte-macrophage colony-stimulating factor (GM-CSF), or pathogen-associated molecular patterns like lipopolysaccharides (LPS). Conversely, alternatively activated M2 MΦs secrete IL10, VEGF, MMPs, thereby dampening proinflammatory responses and inducing wound healing, tissue remodeling, and angiogenesis. Furthermore, they stimulate an immunosuppressive T-cell phenotype (Th2) and inhibit Th1 responses. M2 polarization is induced by IL4 and IL13 or alternatively by IL10. MΦ polarization is a highly dynamic process

allowing them to change their activation status in response to cytokines, apoptotic/necrotic cell derived factors, T-cell interactions, or microenvironmental conditions such as hypoxia [24].

2.2.3 Tumor-associated macrophages in breast cancer

MΦs represent the bulk of the immune cell infiltrate in breast tumors. In contrast to resident MΦs in healthy tissues, they mainly originate from circulating blood monocytes (MOs) that differentiate into MΦs upon extravasation into tissue. Such tumor-associated macrophages (TAMs) can exert several protumorigenic functions and are typically associated with tumor progression and poor prognosis [23]. They exhibit a M2-like or mixed phenotype, however, a minor subpopulation showing a M1-like phenotype can often be detected in tumors. It is important to acknowledge that the above described M1/M2 activation states represent two extremes along a continuum of observed MΦ phenotypes. For TAMs, this simplified terminology is used in order to roughly distinguish phenotypes associated with tumoricidal (M1-like) or tumor supporting (M2-like) functions without the claim to adequately reflect the existing phenotypical plasticity [25]. The recruitment of MΦs to the tumor site and their functional properties are the result of different factors deriving from tumor as well as from stromal cells. In breast cancer, most of the chemoattractive potential for MΦs can be attributed to C-C chemokine ligand 2 (CCL2) and CCL5, secreted mostly by tumor cells, but also by stromal cells. In response to CCL2 and CCL5, recruited MΦs promote migration, angiogenesis, and further recruitment of leukocytes by secreting MMP9, IL8, VEGF, and additional CCL2 and CCL5. TAMs prevalently accumulate in hypoxic regions. Hypoxia further induces protumorigenic functions like VEGF upregulation leading to increased angiogenesis. Since VEGF was shown to mediate MΦ chemoattraction, this might result in a positive feedback which amplifies not only their recruitment but also a protumorigenic shaping of the whole tumor microenvironment. TAMs can further support such an immunosuppressive tumor microenvironment by suppressing cytotoxic T cell responses via secretion of IL10 and TGFβ as well as by recruiting myeloid-derived suppressor cells and regulatory T-cells.

2.2.4 CCL5

The chemokine CCL5, also known as RANTES (regulated upon activation, normal T-cell expressed and secreted) is normally expressed in bronchial epithelium, platelets

and several immune cell populations, yet being inducible in many other cells. It binds to the C-C chemokine receptors (CCRs) 1, 3, and 5, which again are present in various cell types. CCL5 is involved in several inflammatory processes and diseases such as asthma, atherosclerosis, or systemic lupus erythematosus where it induces leukocyte activation and recruitment.

CCL5 upregulation is a common feature in tumors and cancer cell lines and its contribution to immune cell recruitment and tumor invasiveness was confirmed in several *in vivo* as well as in *vitro* models and further substantiated by clinical observations. These effects are primarily assigned to the infiltration of MΦs and the resulting downstream effects, as CCL5 induces expression of MMP9, IL8, and VEGF in these cells. TAM recruitment by CCL5 can lead to amplifying feedback loops at several levels. Cancer cell derived CCL5 stimulates TAMs to produce additional CCL5, its receptor CCR1, as well as other MΦ attracting factors such as CCL2, CCL3, and CCL4. Moreover, TAM derived TNFα can promote CCL5 expression in breast cancer cells [26]. CCL5 promotes metastatic processes, not only as a consequence of MMP9 and IL8 upregulation, but also in a direct manner, as cancer cells often express CCL5 receptors [27]. In breast cancer, hypoxia induces cancer cell migration as a consequence of CCL5 and CCR5 induction [28]. Furthermore, cancer cells are able to stimulate their migratory potential by inducing CCL5 expression in stromal cells, as shown for CAFs and mesenchymal stem cells. Such stimulation of stromal CCL5 expression might also be relevant for establishing the metastatic microenvironment. Besides MΦs, CCL5 was also reported to recruit immature dendritic cells, eosinophils, $CD4^+$ as well as regulatory T-cells to tumor sites, e.g. in classical Hodgkins lymphoma [29]. In ovarian carcinoma, CCL5 was associated to the influx of regulatory T cells into the peripheral inflamed tissue, leading to repression of antitumorigenic T-cell responses. Similar effects can also be brought about by the CCL5 dependent induction of IL10 in TAMs. CCL5 is highly expressed in breast cancer cells, both at primary as well as at metastatic sites, while being poorly expressed in non-neoplastic breast epithelial duct cells [29]. CCL5 expression correlates with MΦ infiltration and tumor progression as well as invasiveness, for example in triple-negative breast cancer [30]. Furthermore, CCL5 inhibition resulted in reduced MΦ infiltration and tumor size in a murine breast cancer model [31]. CCL5 indirectly contributes to angiogenesis by stimulating VEGF and IL8,

but might also be able to directly promote angiogenesis by attracting endothelial cells [32].

2.2.5 Regulation of CCL5

In most cellular contexts, the expression of CCL5 is stimulus dependent. For instance, epithelial cells, fibroblasts, or myeloid cells secrete CCL5 in response to proinflammatory factors like TNFα or IL1β [33]. Since CCL5 plays a prominent role in virus defense, viral particles are also strong and well-studied inducers of CCL5 expression [34]. Furthermore, hypoxia was described to induce CCL5 in a hypoxia-inducibel factor 1 alpha (HIF1α) dependent manner [28]. Such stimuli mostly affect CCL5 transcription. The underlying mechanisms and involved transcription factors differ and are strongly dependent on the cellular context (table 1). Transcriptional regulation of CCL5 was studied in different cellular models and shown to be dependent on a clearly defined promoter region adjacent to the transcription start site. This promoter contains several so far identified transcription factor response elements including binding sites for peroxisome proliferator-activated receptor gamma (PPARγ), cAMP response element-binding protein (CREB), activator protein 1 (AP1), interferon regulatory factors (IRFs), krueppel-like factor 13 (KLF13), CCAAT enhancer binding proteins (C/EBPs), and NF-κB (nuclear factor kappa-light-chain-enhancer of activated B cells) [35, 36]. CCL5 was first identified in T-cells as a factor induced several days after T-cell receptor activation [37]. In naïve T-cells, the genomic CCL5 locus is in a heterochromatin conformation and consequently, the promoter is transcriptionally silent. CCL5 activation requires the assembly of an enhanceosome complex, which includes p50/p65 binding to the NF-κB element and CREB/ATF/jun-D binding to the CRE site. This complex mediates chromatin remodeling and transcription initiation. The central factor for the assembly of the enhanceosome is KLF13 (aka RFLAT1), which binds to the first NF-κB site (-71 to -53) [38]. KLF13 protein expression is restricted to activated T-cells and its induction kinetics correlate with CCL5 expression in these cells [39].

Table 1: Transcriptional regulation of CCL5

Cell type [reference]	**Stimulus**	**Transcription factor and effect on CCL5**	**Promoter element(s) or region**
Monocytes [40]	-	YB1 ↑	-28 to -10
Macrophages [38]	-	YB1 ↓	-28 to -10
Endometrial stromal cells	TNFα	PPARγ ↑ (?)	-334 to -332
Astrocytes	IL1 + IFNβ	C/EBPβ↑	C/EBP (+ISRE, AP1)
Cancer cells	-	c-Jun ↑	CRE
Epithelial cells	*Helicobacter pylori* infection	Various ↑	CRE, ISRE, C/EBP and NF-κB
Macrophages	LPS	ATF, Jun ↑	CRE/AP1
Breast cancer cells	-	AP1 (c-Jun) ↑	CRE/AP1
Various	RNA viruses	IRFs ↑	ISRE
Fibroblasts, myeloid cells	*Helicobacter pylori* infection	IRF3/IRF7 + NF-κB ↑	ISRE, NF-κB
Cancer cells	-	NF-κB ↑	NF-κB
NK cells	-	SP1 ↑	NF-κB
Renal tubular cells	- (?)	NF-κB (p65/p65 dimer) ↑	NF-κB
Cancer cells	IL6 (only prolonged)	Unphosphorylated p65/p50/Stat3 ↑	NF-κB

In other tissues, the most relevant transcription factor for CCL5 expression is NF-κB, which is a key regulator in many inflammatory processes as well as tumorigenesis. The list of NF-κB target genes includes inflammatory factors like TNFα, IL1, IL6, IL8, and cyclooxygenase 2 (COX2) as well as tumor promoting factors like B-cell lymphoma extra large (Bcl-xL), VEGF, Cyclin D1, or MMP9 [41]. NF-κB is involved in many CCL5 regulating processes, either exclusively or in cooperation with other transcription factors. Furthermore, constitutive expression of CCL5 in cancer cells was predominantly attributed to increased NF-κB activity, however also elevated c-Jun N-terminal kinase (JNK) and mitogen-activated protein kinase (MAPK) signaling, leading to binding of c-Jun to the CRE, was reported to be crucial in this context [30].

Interestingly, it was shown that prolonged signal transducer and activator of transcription 3 (Stat3) signaling can lead to CCL5 activation by an unconventional NF-κB complex consisting of unphosphorylated, i.e. usually inactive, p65/p50 and unphosphorylated Stat3. This mechanism was proposed to allow for prolonged CCL5 expression after TNFα stimulation, caused by the TNFα dependent induction of IL6, which maintains Stat3 activation by an autocrine feedback loop [42].

2.3 HuR

mRNAs never appear as naked molecules but are always accompanied by RNA binding proteins (RBP), which are involved in all steps of mRNA maturation as well as its intracellular transport, turnover, and translation [43]. The regulation of these interdependent processes allows for several co- and post-transcriptional mechanisms by which RBPs may influence the translatome. Here, the two typical ways are the regulation of mRNA decay and translation efficiency. The stability of a mRNA or rather its half-life is determined by destabilizing factors that mark the mRNA for degradation [44]. Translation efficiency can be directly modulated by altering the activity of the translation machinery or indirectly inhibited by mRNA sequestration in stress granules or mRNA processing bodies [45].

2.3.1 Structure and functions of HuR

The RBP human antigen R (HuR), also known as embryonic lethal abnormal vision-like 1 (ELAVL1), is one of the best studied factors for the regulation of mRNA stability. Contrary to the primarily destabilizing functions of other RBPs, it has the exceptional characteristic to mainly stabilize mRNAs. Additionally, HuR also regulates translation and may have further functions linked to its RNA binding capacity [46].

HuR is the only ubiquitously expressed member of the family of Hu RBPs, whose other 3 members are less familiar due to their neuron restricted expression [47]. While the Hu labeling dates back to their first identification as common antigens of the paraneoplastic encephalomyelitis associated Hu antibody, the ELAVL nomenclature refers to their homology to the *Drosophila* ELAV protein [48, 49]. The Human Genome Organisation (HUGO) Gene Nomenclature Committee (HGNC) defines ELAVL1 as the official nomination [50], however, HuR is clearly the more conventional name when referring to the protein.

The HuR protein has a molecular weight of 36 kDa, correlating with the 326 amino acids long sequence, and contains 3 RNA recognition motifs (RRM) plus a hinge region between RRM2 and RRM3 specified as HuR nucleo-cytoplasmic shuttling (HNS) domain [51].

HuR recognizes and binds adenylate/uridylate (AU)- and U-rich elements (AREs), which are typical binding elements for regulators of mRNA stability, estimated to be present in 5-8% of all eukaryotic mRNAs with most of them located in the 3‘ untranslated region (UTR) [52]. Apart from HuR, 19 further ARE-binding proteins (AUBP) are known to date, with tristetraprolin (TTP), AU-rich element RNA-binding protein 1 (AUF1), and KH-type splicing regulatory protein (KSRP) being the most notable ones in the context of mRNA stability regulation [53].

2.3.2 Molecular mechanisms of HuR functions

As briefly outlined above, the functions of HuR are not restricted to mRNA stabilization. Especially translational regulation by HuR is commonly observed [54]. In this case, there is no preference for up- or downregulation and the HuR binding sites can be found in the 3‘UTR, as seen for p53 or cytochrome c, or in the 5‘UTR, as seen for IGF-IR [55]. HuR may also play a role in IRES-dependent translation, e.g. it was shown that IRES-dependent translation of p27 can be inhibited by HuR [56]. HuR can further affect protein expression levels by enhancing mRNA shuttling leading to cytoplasmic mRNA accumulation, as shown for CD83 [57]. Interestingly, the binding site in this case was located in the mRNA coding region.

RBPs are only one side of the machinery that regulates mRNA stability and translation. The other side is represented by micro RNAs (miRNAs) that have exclusive as well as overlapping binding sites on targeted mRNAs and act as negative regulators in both processes. The interplay of HuR and miRNAs can lead to various results. For instance, they can counteract each other by competitive binding to overlapping sites [58]. However, interaction with miRNAs may also facilitate further functionalities of HuR, as shown for c-Myc, which is repressed upon let-7 miRNA recruitment by HuR [59]. Similar effects can also be observed for the co-binding of HuR with other RBPs like AUF1, in this case leading to p16 mRNA degradation [60]. Since the RNA binding capability is not limited to mRNAs, HuR also has the ability to directly bind to miRNAs. It is considered being able to repress miRNA functions by acting as a miRNA sponge, similar to the miRNA sequestration functions of some

lncRNA. This is based on the observation that HuR can counteract the translation repression of PDCD by miRNA-21 [61]. Notably, in this process, HuR as well as miRNA-21 are bound to the PDCD4 3‘UTR but at separate sites. In the nucleus, HuR might have additional functions associated with mRNA processing as it was demonstrated that binding to the pre-mRNA of Fas regulates alternative splicing and thereby the switch between soluble and transmembrane isoforms of Fas [62].

2.3.3 HuR and cancer

The linkage of Hu proteins to cancer was already established by their first identification as antigens in tumor patients [63]. HuR protein is overexpressed in many cancer types while there exist conflicting data concerning altered mRNA levels in tumor tissue. In clinical tumor samples, cytoplasmic protein levels or the proportion of cytoplasmic to nuclear abundance is often used as an indicator for general HuR activity since the main function of HuR as a regulator of mRNA stability and translation requires its translocation from the nucleus to the cytoplasm [64]. Cytoplasmic expression patterns appear as a negative prognostic marker for survival in oral, esophageal, gastric, gallbladder, renal, urothelial, lung, breast, and ovarian cancer [65].

With regard to the hallmarks of cancer, HuR appears to be involved in almost all of these processes [66]. The growth promoting function of HuR is one of its most consistently observed characteristics. HuR contributes to cell cycle deregulation in cancer by upregulating Cyclin A2, B1, D1, and E1, and was shown to inhibit the IRES-mediated translation of the growth suppressor p27 [54]. Furthermore, HuR increases several proangiogenic factors like VEGF, IL8, and COX2 [67]. It also enhances translation of HIF1α, which regulates cellular adaptations to hypoxia, including transcriptional induction of VEGF [68]. A contrary phenotype was reported in an orthotopic breast cancer xenograft model, where HuR overexpression strongly impaired tumor growth as a consequence of antiangiogenic signaling involving upregulation of thrombospondin 1 (TSP1) [69]. Interestingly, another study suggests that this feature gets lost during malignant progression in the course of global changes in HuR-bound mRNAs [70]. HuR further facilitates the miRNA-mediated repression of c-Myc. Constitutive overexpression of this oncogene leads to several protumorigenic effects, however, the repressive function of HuR was also speculated

to act in a tumor supporting manner as hyperactive c-Myc signaling can trigger apoptosis [71, 72].

2.4 Aims of this study

The aim of my work was to study the influence of HuR on cancer-immune cell interactions in breast carcinoma. For this purpose, I initially established and characterized HuR dependent changes in MCF-7 breast cancer spheroids. To assess the potential role of tumor HuR on infiltrating immune cells, I further analyzed the influence of HuR on cytokine/chemokine expression in tumor spheroids. Subsequently, I determined the underlying regulatory principles for one of the newly identified HuR targets in this context – CCL5. The functional implications of this regulation were further evaluated in a co-culture setting of tumor spheroids and primary monocytes. Finally, bioinformatics analyses of publically available breast tumor data sets were carried out to support the translatability of my findings to a clinical context.

3 Materials and Methods

3.1 Materials

3.1.1 Cells

Primary human monocytes

Primary MOs were isolated from human buffy coats obtained from DRK-Blutspendedienst Baden-Württemberg-Hessen (Institut für Transfusionmedizin und Immunhämatologie, Frankfurt, Germany)

Human cell lines

All cell lines (listed in table 2) came from ATCC-LGC Standards (Wesel).

Table 2: Human cell lines

Name	Origin
MCF-7	Breast carcinoma
MDA-MB-231	Breast carcinoma
MDA-MB-468	Breast carcinoma
A549	Lung carcinoma
T98G	Glioblastoma
A375	Malignant melanoma
HEK293T	Variant of the embryonic kidney cell line HEK293 additionally expressing the SV40 large-T-antigen

Bacteria

Competent bacteria strains were obtained from Agilent Technologies (Waldbronn). XL10-Gold ultracompetent cells were used for amplification of mutated vectors generated with the QuikChange XL II site directed mutagenesis kit. XL1-Blue super competent bacteria were used for general vector amplification.

3.1.2 Oligonucleotides

Primers were purchased from Biomers.net (Ulm). All nucleotide sequences are depicted in 5'-3' orientation.

Table 3: Primer pairs for qPCR

Target	Forward sequence	Reverse sequence
Actin	AGCCTCGCCTTTGCCG	CTCGTCGCCCACATAGGAAT
C/EBPβ	AACTCTCTGCTTCTCCCTCTG	AAGCCCGTAGGAACATCTTT
CCL28	TGTGACTTGGCTGCTGTCAT	TCCCCTGATGTGCCCTGTTA
CCL5	GAAATGGGTTCGGGAGTACAT	AGGACAAGAGCAAGCAGAAA
HuR	ACCCGGTTTGCTTCCAAATGAAGG	AGGCCTCCTGTCAGCTGAATTCTT
IGFBP4	ATCATCCCCATCCCCAACTG	GGTCCACACACCAGCACTT
IFNβ	ACTGCAACCTTTCGAAGCCT	AGCCTCCCATTCAATTGCCA
IL6	TCAATGAGGAGACTTGCCTGGTGA	TACTCATCTGCACAGCTCTGGCTT
IRF1	AGGAGGGGACATTCCTGTCA	AGCCGTGAGGACCTTTCTTG
IRF2	CCTCAGAACGGACGAGATAATG	AGATAAGGTGCAGAAGCAGAC
IRF3	GCAAAGAAGGGTTGCGTTTAG	CCTGAGTTCACAAACTCGTAGAT
IRF5	GAGCTCAGCTTGGTCCCG	GGATGGACTGGTTCATGGCA
IRF7	CGCCACTGTTTAGGTTTCGC	GCTGCCTCGGTATGGATCTC
IRF8	CGAGGTTACGCTGTGCTTTG	AATCGTCCACAGAAGGCTCC
IRF9	AACTCAGGATGGCATCAGGC	GTCTTCCAGACAGCTGGACC
ISRE (ChIP)	GCTCACTCTAGATGAGAGAG	CCCTTTATAGGGCCAGTTGAG
Nucleolin	GACAGAAGCTGATGCAGAGAAAACC	CACTCCAAGTGCTATTCTTTCCACC

Table 4: Primers for In-Fusion cloning

Primer	Sequence
prom for	TATCGATAGGTACCGACAGTGGAATAGTGGCTGG
prom +5UTR rev	TTGGCGTCTTCCATGGTACCTGTGGGAGAGGCT
prom -5UTR rev	CCGGAATGCCAAGCTTCAGGCTGGCCCTTTATAG
-350 for	TATCGATAGGTACCGTAATAAAGACTCAGTGACTTC
-220 for	TATCGATAGGTACCGTTTTCCACCATTGGTGCTTG
-140 for	TATCGATAGGTACCGCTCGAATTTCCGGAGGCT
-90 for	TATCGATAGGTACCGCACTTATGATACCGGCCAA

3.1.3 Plasmids

Table 5: Plasmids (commercially available)

Plasmid	Description	Provider
pGL3-basic	*firefly* luciferase reporter vector without promoter	Promega*
pRL-SV40	*renilla* luciferase reporter vector under control of a SV40-promoter	Promega
pCMV-dR8	lentiviral packaging plasmid	Sigma Aldrich[#]
pMD2.G	lentiviral envelope plasmid	Sigma Aldrich
pLKO.1-puro shHuR1	lentiviral transfer plasmid for shRNA against HuR (TRCN0000017273)	Sigma Aldrich
pLKO.1-puro shHuR2	lentiviral transfer plasmid for shRNA against HuR (TRCN0000017276)	Sigma Aldrich
pLKO.1-puro shCTRL	lentiviral transfer plasmid for non-target shRNA (SHC002)	Sigma Aldrich

*(Mannheim) [#] (Steinheim)

Reporter constructs generated in this study (listed in table 6) are based on the pGL3-basic vector.

Table 6: Generated reporter plasmids

Plasmid	Insert
pGL3-CCL5prom+5UTR	880 bp upstream of the CCL5 ORF, including the 5'UTR and the promoter region
pGL3-CCL5prom	812 bp upstream of the CCL5 TSS, hereinafter be referred as the core promoter
pGL3-prom350	350 bp upstream of the CCL5 TSS, promoter fragment
pGL3-prom220	220 bp upstream of the CCL5 TSS, promoter fragment
pGL3-prom140	140 bp upstream of the CCL5 TSS, promoter fragment
pGL3-prom90	90 bp upstream of the CCL5 TSS, promoter fragment
pGL3-Δ135-120	modified core promoter, lacking nucleotides 135-120 upstream of the CCL5 TSS
pGL3-mut114-107	modified core promoter, nucleotides in the indicated region (TTTCTTTT) were changed to AAACAAAA
pGL3-Δ101-94	modified core promoter, lacking nucleotides 101-94 upstream of the CCL5 TSS
pGL3-Δ71-40	modified core promoter, lacking nucleotides 71-40 upstream of the CCL5 TSS

3.1.4 Antibodies

Antibodies for Western Blot (WB), flow cytometry (FC), neutralization studies (NEU), immunohistochemistry (IHC), and chromatin immunoprecipitation (ChIP) are listed in table 7.

Table 7: Antibodies

Antibody against	Provider	Application
Nucleolin	Santa Cruz (Heidelberg)	WB
HuR	Santa Cruz	WB
β-tubulin	Sigma Aldrich (Steinheim)	WB

histone H3	Millipore (Schwalbach)	WB
Stat1	Millipore	WB
IRF1	Santa Cruz	WB, ChIP
IRF3	Santa Cruz	WB
pIRF3	Cell Signaling (Frankfurt)	WB
IRF5	Abcam (Cambridge, UK)	WB
IRF9	Santa Cruz	WB
KI-67	Biomol (Hamburg)	IHC, FC
Hypoxyprobe-1	Chemicon (Temecula, USA)	IHC
CCL5	R&D Systems (Wiesbaden)	NEU
IFNAR2	Acris (Herford)	NEU
mouse (IgG2a isotype control)	Acris	NEU (IFNAR)
goat (IgG isotype control)	Santa Cruz	NEU (CCL5)
mouse/goat/rabbit (IRDye 680LT)	Li-COR (Bad Homburg)	WB
mouse/goat/rabbit (IRDye 800CW)	Li-COR	WB
cleaved caspase-3 FITC-coupled	BD Biosciences (Heidelberg)	FC

3.1.5 Solutions and compounds for cell culture

High glucose DMEM was obtained from Gibco (Carlsbad), FBS was purchased from Capricorn (Ebsdorfergrund) and antibiotic additives came from Sigma Aldrich (Steinheim). All other media, media supplements and ready-to-use solutions for cell culture were obtained from PAA (Cölbe).

3.1.6 Chemicals, reagents, compounds and kits

Chemicals were usually purchased from Sigma Aldrich, Roth or Merck and in the grade of purity required for the respective experimental purpose (at least ACS grade). Special chemicals, reagents and kits are listed in table 8.

Table 8: Chemicals, reagents and kits

Product	**Provider**
Coelentherazine	Promega (Mannheim)
Counting Beads (Flow-Count Fluorospheres)	Beckman Coulter (Krefeld)
C-Series Human Antibody Array	RayBiotech (Norcross, USA)
DC Protein Assay Kit	BioRad (München)
Dithiothreitol	AppliChem (Darmstadt)
D-Luciferin	AppliChem
DNA loading dye	New England Biolabs (Frankfurt)
Fluoromount G	SouthernBiotech (Birmingham, USA)
GeneRuler DNA ladder	Invitrogen (Darmstadt)
GenMute transfection reagent	SignaGen (Rockville, USA)
Human CCL5 Flex Set	BD Biosciences (Heidelberg)
Human CD14 microbeads	Miltenyi Biotec,(Bergisch Gladbach)
Human FcR binding inhibitor	eBioscience (Frankfurt)
In-Fusion HD Cloning Kit	Clontech (Mountain View, USA)
iQ SYBR Green Supermix	Biorad (München)
JetPrime	Peqlab (Erlangen)
Lymphocyte separation medium (Ficoll)	PAA Laboratories (Cölbe)
Maxima First Strand cDNA synthesis kit	Thermo Fischer (Schwerte)
Nonidet P-40 (NP-40)	ICN Biomedicals (Eschwege)
NucleoBond Xtra Maxi Kit	Macherey-Nagel (Düren)
NucleoSpin Gel and PCR Clean-up Kit	Macherey-Nagel
NucleoSpin Plasmid Kit	Macherey-Nagel

Passive lysis buffer 5x	Promega
PeqGold RNAPure	Peqlab
Phosphate buffered saline (PBS)	Biochrom (Berlin)
Phosphostop	Roche Diagnostics
Phusion High-Fidelity DNA Polymerase	New England Biolabs (Frankfurt)
Protease Inhibitor Mix (PIM)	Roche Diagnostics (Grenzach)
Protein A Sepharose CL-4 beads	Sigma Aldrich (Steinheim)
QIAquick PCR purification kit	Qiagen (Hilden)
Quikchange XL II Kit	Agilent (Waldbronn)
Restriction enzymes	New England Biolabs
Rotifect	Roth (Karlsruhe)
Sepharose CL-4B beads	Sigma Aldrich
Taq DNA Polymerase	Invitrogen

3.1.7 Instruments

Table 9: Instruments

Product	**Provider**
12-channel Eppendorf Research (200 µL)	Eppendorf (Hamburg)
Apollo-1 LB 911 photometer	Berthold Technologies (Bad Wildbad)
Autoclave HV 85	BPW (Süssen)
AutoMACS™ Separator	Miltenyi Biotec (Bergisch-Gladbach)
AxioCam MRm	Carl Zeiss Micro Imaging (Jena)
Axioskop 40 microscope	Carl Zeiss (Göttingen)
AxioVert 200M fluorescence microscope	Carl Zeiss Micro Imaging

B250 Sonifier	Branson Ultrasonics (Danbury, USA)
Bacteria clean bench	Heraeus (Hanau)
Bacteria incubator B5042	Heraeus
Bacteria incubator Innova®44	New Brunswick Scientific (Nürtingen)
Centrifuge 5415 R and 5810 R	Eppendorf (Hamburg)
CFX96 Real-time PCR	BioRad
Hera cell 150 (Lamina)	Thermo Fisher (St. Leon-Rot)
IncuCyte Zoom	Essen BioScience (Ann Arbor, USA)
LabLine Orbit Shaker	Uniequip (Martinsried)
LSRII Fortessa	BD Biosciences (Heidelberg)
Magnetic stirrer Combimag	RCH IKA Labortechnik (Staufen)
Mastercycler	Eppendorf
Mini-PROTEAN 3 System	BioRad (München)
Mithras LB 940 luminometer	Berthold (Bad Wildbad)
NanoDrop ND-1000	Peqlab Biotechnologie (Erlangen)
Neubauer counting chamber	Labor Optik (Friedrichsdorf)
Odyssey infrared imaging system	Li-COR (Bad Homburg)
Optima L 90K Ultracentrifuge	Beckman Coulter (Krefeld)
Pipetboy	Hirschmann Laborgeräte (Eberstadt)
Pipettes (10 µL, 100 µL, 1,000 µL)	Eppendorf
Pressure cooker vitafit	Fissler (Idar-Oberstein)
PurelabPlus Pure water system	ELGA LabWater (Siershahn)
Roller Mixer SRT1	Bibby Scientific Ltd. (Staffordshire, UK)
Thermomixer compact	Eppendorf
Tissue embedding system EG1150H	Leica (Wetzlar)

Trans-Blot SD blotting machine	BioRad

3.1.8 Software

Table 10: Software

Product	**Provider**
AxioVision Release 4.7	Carl Zeiss (Göttingen)
Bio-Rad CFX Manager 3.1	Bio-Rad (München)
Corel Draw X5	Corel Corp. (Ottawa, Canada)
Endnote X6	Thomson Reuters (Carlsbad, USA)
FACS Diva	BD Biosciences (Heidelberg)
Image Studio Lite	Li-COR (Bad Homburg)
MikroWin 2000	Berthold Technologies (Bad Wildbad)
MSOffice 2010	Microsoft Deutschland (Unterschleißheim)
Nano Drop 1000 3.8.1	Thermo Fisher (Schwerte)
Odyssey 2.1	Li-COR
Photo Read V1.2.0.0	Berthold Technologies

3.2 Methods

3.2.1 Cell culture

Human cell lines were maintained in high glucose DMEM supplemented with 10% fetal calf serum (FCS), 100 U/mL penicillin and 100 µg/mL streptomycin. Medium of transduced cells additionally contained 2 µg/mL puromycin dihydrochloride. Cells were kept at 37°C in a humidified atmosphere with 5% CO_2 and transferred before reaching full confluency. Cells were regularly tested for mycoplasma contamination.

3.2.2 Proliferation measurement

5 x 10^3 MCF-7 cells per well were seeded in a 96-well plate and confluency was automatically determined every 3 h by an IncuCyte Zoom (Essen BioScience, Ann Arbor, USA).

3.2.3 Lentiviral transduction

Stable HuR knockdown cells (sh HuR) were generated by lentiviral transduction using a set of 5 different shRNA constructs. Parallely generated cells expressing a non-target shRNA (sh ctrl) served as negative control. Lentiviral transduction particles were produced in HEK293T cells by co-transfection of pMD2.G, pCMV-dR8 and the specific transfer vectors (JetPrime transfection protocol). After 72 h, supernatants containing lentiviral particles were filtered and stored at -80°C until use.

3.2.4 Isolation of CD14-positive human monocytes

Peripheral blood mononuclear cells were collected from human buffy coats by density gradient centrifugation using Biocoll Separating Solution. After two washing steps with leukocyte running buffer, cells were resuspended in 200 mL leukocyte running buffer. After adding 50 µL CD14 microbeads, cells were incubated on ice for 15 min and applied to the autoMACS cell sorter (program: possel)

3.2.5 Spheroid formation and monocyte co-culture

Multicellular spheroids were generated according to the liquid overlay technique by seeding 5 x 10^3 MCF-7 cells per well in agarose-coated 96-well plates, followed by centrifugation at 500 g for 3 min. Medium was exchanged after 5 days of incubation. For co-culture experiments, 5 days old spheroids were co-cultured with 1 x 10^5 $CD14^+$ MOs for additional 2 days. For the determination of MΦ infiltration, spheroids were washed twice with PBS, digested with Accutase, incubated with Fc block and anti CD14 antibody and measured by flow cytometry using a LSRFortessa flow cytometer and FACS Diva software (BD Biosciences).

3.2.6 Monocyte migration assay

Freshly isolated MOs were suspended in FCS-free medium and seeded onto transwell polycarbonate 5 µm membrane cell culture inserts (5 x 10^5 cells per insert). Inserts were then quickly transferred to cell culture compartments containing supernatants of 7 day old spheroids. After 90 min, inserts were removed and migrated MOs in the lower compartment were counted using a Neubauer counting chamber.

3.2.7 Subcellular fractionation

MCF-7 cells were lysed in 150 µL cytosol buffer for 15 min, followed by addition of 10 µL NP-40 (10%) and thorough vortexing. After centrifugation at 12,000 g for 5 min, the supernatant containing the cytosolic fraction was harvested. After three washing steps with PBS, the pellet containing the nuclear fraction was resuspended in 70 µL SDS lysis buffer and sonicated for 15 x 1 s. Anti-β-tubulin and anti-Histone H3 were used as loading controls in following western analyses.

3.2.8 Western analysis

MCF-7 cells were lysed in lysis buffer and sonified. 60 µg protein were separated by SDS-PAGE and transferred onto nitrocellulose membranes. Membranes were incubated with given primary and secondary antibodies and proteins were visualized on an Odyssey infrared imaging system (Li-COR Biosciences).

3.2.9 Cytokine Array

Spheroid lysates from 3 experiments with equalized protein concentration were pooled and analyzed using a RayBio C-Series Human Cytokine Antibody Array 2000 Kit according to the manufacturer's protocol. Signals were detected by incubating the membrane with Super ECL for 5 min and subsequent exposure to x-ray films. Films were scanned and analyzed with Image Studio Lite software. Relative protein concentrations were quantified after background substraction (blank value spots (-)) and membrane-to-membrane equalization (positive control spots (+)).

3.2.10 Cytometric bead array

Cytometric bead array (CBA) was performed using a CCL5 Flex Set and measured by flow cytometry using a LSRFortessa flow cytometer and FACS Diva software (BD Biosciences). Compatibility of CBA detection with protein lysis buffer was successfully demonstrated by measuring the protein standard curve in lysis buffer and comparing the results to a standard curve in CBA buffer. For measurement of CCL5 levels in spheroid lysates, equal amounts of protein were applied to to the CBA by first equalizing the protein concentration in the samples and then applying equal volumes, corresponding to 60 µg protein.

3.2.11 Quantitative real-time PCR

Total RNA was extracted from MCF-7 cells using PeqGold RNAPure Kit and reverse transcribed using the Maxima First Strand cDNA synthesis kit. For quantitative analyses, individual mRNAs were subsequently analyzed by real-time PCR using specific primers and the iQ SYBR Green Supermix. Real-time PCR results were quantified using the Biorad CFX Manager with actin and nucleolin expression as internal control.

3.2.12 Chromatin Immunoprecipitation (ChIP)

For chromatin cross-linking, MCF-7 cells from five 15 cm dishes (2 x 10^7 each) were treated with 1% formaldehyde at 37°C. After 10 min, the reaction was stopped by adding 0.125 M glycine and cells were collected after two washing steps with PBS followed by centrifugation (5 min at 500 rpm, 4°C). Cells were resuspended in 1.5 mL

L1 buffer and lysed by addition of 250 µL L1B buffer (L1 + 1% Nonidet P-40) and incubation on a roller mixer at 4°C for 15 min. Nucleic protein was resuspended using L2 buffer and cross-linked chromatin was sheared to an DNA fragment size of around 200 – 500 bp by sonification on ice (8 - 12 steps at 10% intensity/1s, proper DNA fragment size was controlled for each experiment by gel electrophoresis). After centrifugation (5 min at 13000rpm and 4°C), 5% of the supernatant was collected and used as input sample in the PCR analysis, the remaining sample was precleared with Sepharose CL-4B beads and equal amounts of chromatin were incubated overnight with antibodies against IRF1, H3 and the respective IgG isotype controls. Immunocomplexes were recovered by 2 h incubations with protein A-Sepharose CL-4 beads at 4°C, followed by reversed cross-linking. For DNA purification, a QIAquick PCR purification kit (Qiagen) was used according to the manufacturer's instructions. Enrichment of specific DNA fragments in the immunoprecipitated material was determined by qPCR.

3.2.13 Plasmid construction

CCL5 promoter reporter vectors were generated by amplifying a putative core promoter, i.e. 812 nucleotides upstream of the CCL5 transcription start site from genomic MCF-7 DNA, using primers designed for direct insertion into the pGL3-Basic backbone (prom for and prom +5UTR rev, sequences see Table 4). The product was then inserted into the pGL3-Basic vector using the In-Fusion Cloning system (Clontech). Mutations were introduced using the Quikchange Kit (Agilent) according to the manufacturer's instructions.

3.2.14 Luciferase reporter assay

MCF-7 cells were transiently co-transfected with pGL3-Basic vector containing the indicated promoter sections and pRL-SV40 using Rotifect according to the manufacturer's protocol. After 2 days, cells were lysed by shock-freezing (liquid nitrogen) in passive lysis buffer (Promega) and *firefly* and *renilla* luciferase activities were determined using a Dual Luciferase kit assay on a Mithras LB 940 luminometer (Berthold, Bad Wildbad, Germany).

3.2.15 Statistical analysis

Unless indicated differently, data are presented as mean values ± SEM of at least five independent experiments. Statistical analyses were performed using Student's t-test for paired samples.

4 Results

4.1 Identification of novel HuR targets

Elevated HuR expression or activity has been correlated with malignant progression in a broad variety of different cancer types and HuR was further functionally linked to increased proliferation, apoptosis resistance, angiogenesis, and metastasis in various tumor cell lines. Moreover, HuR was shown to be involved in the regulation of inflammatory factors like COX2, IL8, or CCL2 and therefore may contribute to immunomodulatory processes in tumorigenesis. With the present work, I aimed at characterizing the impact of HuR on the interplay between tumor cells and their immune cell-shaped microenvironment.

4.1.1 Stable knockdown of HuR in MCF-7 cells

To study the role of HuR in the context of ER+ breast cancer, I generated a stable HuR knockdown cell line. Therefore, I introduced two different shRNA constructs into MCF-7 cells via viral transduction. A non-targeting shRNA sequence served as control. Both sequences caused an efficient downregulation of HuR, which remained stable for several weeks of cultivation as shown on RNA as well as protein level (Figure 1). While the mRNA levels of HuR were similar in both cell lines, the sh HuR clone 1 showed a stronger downregulation of HuR protein and was therefore chosen for further analysis.

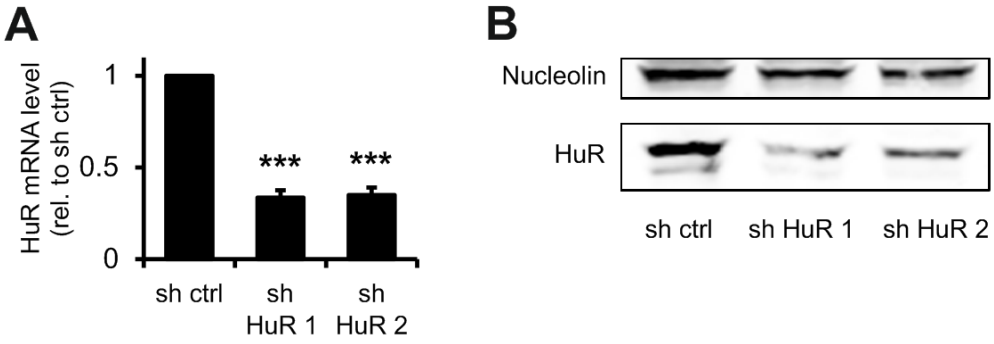

Figure 1: Stable knockdown of HuR in MCF-7 cells
MCF-7 cells stably transduced with two shRNA clones targeting HuR (sh HuR 1 and sh HuR 2) were compared to cells stably transduced with a non-targeting shRNA (sh ctrl). **(A)** HuR mRNA expression was analyzed by qPCR and normalized to actin and nucleolin mRNA levels. Data represent means ± SEM (n > 5; ***p < 0.001). **(B)** HuR protein expression in sh ctrl and sh HuR MCF-7 cells was analyzed by Western blot analysis. Nucleolin served as a loading control. Blot is representative for at least five independent experiments.

To further characterize my cell system, I determined the proliferation rate of HuR knockdown cells. In line with preceding reports, depletion of HuR resulted in attenuated MCF-7 proliferation (Figure 2).

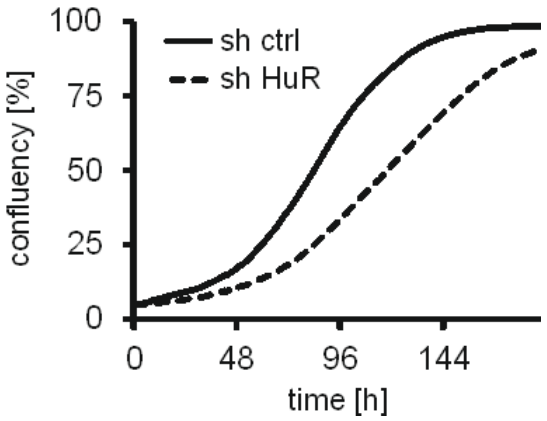

Figure 2: HuR depletion diminishes growth of MCF-7 cells
Sh ctrl and sh HuR MCF-7 cells were grown for indicated time periods. Proliferation rate was determined by confluency measurement in an IncuCyte live cell imaging chamber. Graph is representative for three independent experiments.

4.1.2 3D spheroid culture

Having analyzed the behavior of the HuR deficient cells in a monolayer setup, I next aimed to extend the characterization to more physiologically relevant experimental

settings. As the uniform micromilieu in monolayer cell culture systems differs vastly from the complex environment present in a three dimensional *in vivo* tumor and these microenvironmental conditions appear as a critical determinant for the phenotypic skewing of tumor associated immune cells, I chose a 3D spheroid approach to address the traits of HuR in the context of tumor–immune cell interactions. In such spheroid cultures, proliferation is mainly restricted to cells of the outer layers, while a decreased supply of oxygen and nutrients in the inner region results in the appearance of hypoxia on day 5 and the formation of a necrotic core on day 6 of spheroid growth (Figure 3).

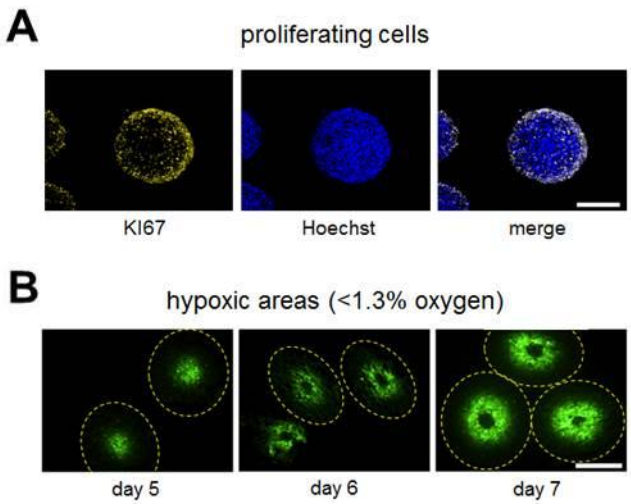

Figure 3: MCF-7 spheroids exhibit distinct microenvironmental characteristics
MCF-7 cells were grown as 3D tumor spheroids and paraffin sections were analyzed at selected time points. **(A)** Immunohistochemical staining of the proliferation marker Ki-67 in spheroids at day 5. **(B)** Fluorescence staining of hypoxic areas with hypoxyprobe in spheroids harvested at days 5 to 7.

As HuR depletion attenuated proliferation of monolayer cells (Figure 2), I first determined if this characteristic also applies to the spheroid system by comparing the diameter of 7 days old spheroids. Indeed, HuR knockdown spheroids exhibited a slight, but significant decrease in size compared to sh ctrl spheroids (Figure 4).

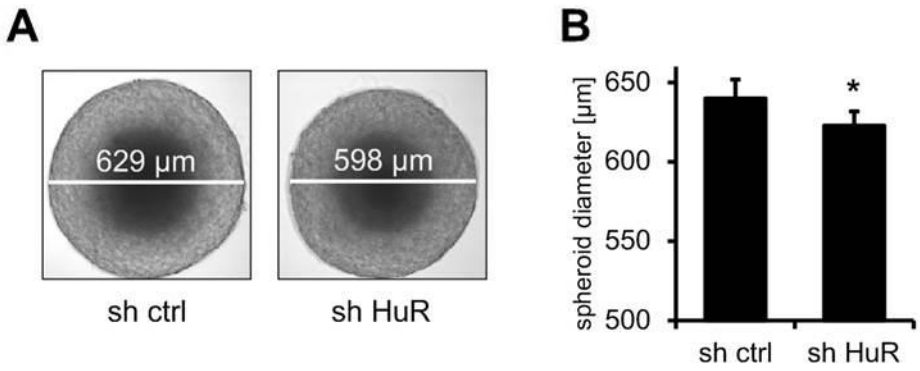

Figure 4: HuR depletion diminishes growth of MCF-7 spheroids
sh ctrl and sh HuR MCF-7 spheroids were grown for seven days. **(A)** Representative picture of the respective spheroids. **(B)** Quantification of spheroid diameters. Data represent means ± SEM (n > 5; *p < 0.05).

Thus, HuR appears to similarly support proliferation of MCF-7 in a complex 3D tumor spheroid setting as under standard monolayer conditions.

4.1.3 Screening for HuR regulated cytokines in spheroids

To assess how HuR affects the tumor microenvironment, I next aimed at identifying novel targets of HuR in the tumor spheroid context. As several features of the *in vivo* tumor microenvironment, such as hypoxia or presence of DAMPs, are known to affect the functional properties of HuR and consequently its specific subset of regulated targets, I focused on the analysis of inflammatory factors in MCF-7 spheroids. To this end, I analyzed tumor spheroid lysates using a protein array, which allows for simultaneous detection of 174 cytokines and chemokines (Figure 5). Densitometric analysis revealed differential presence of various factors in HuR knockdown vs. ctr cells. Interestingly, while HuR has been shown to predominantly act as a positive regulator of target gene expression, the majority of differentially detected proteins were upregulated in HuR knockdown spheroids.

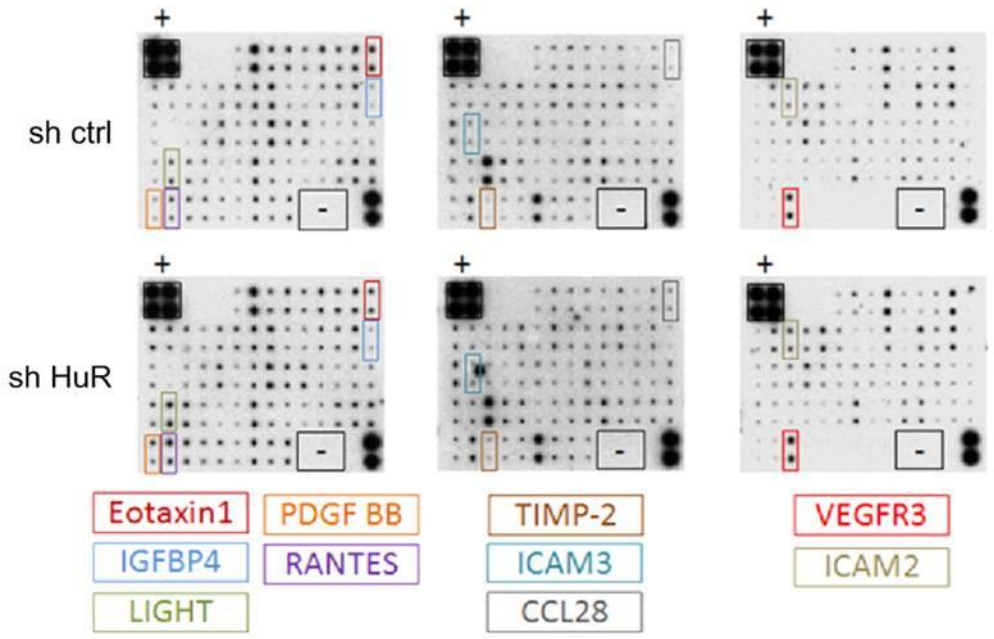

Figure 5: Cytokine array
Protein lysates of sh ctrl and sh HuR spheroids from 3 experiments were pooled and applied to a Raybiotech C2000 cytokine array according to the manufacturer's instructions.

For the following analyses, I selected the factors which showed the highest fold difference and at the same time exhibited a meaningful difference in absolute signal intensities. The resulting set of 10 factors is listed in table 11. As indicated above, the majority of candidates (8 of 10) appeared to be upregulated in sh HuR spheroids, including various CCLs (CCL5, CCL28), growth factors (PDGF BB), and adhesion molecules (ICAM2 and 3).

Table 11: Quantitative analysis for selected factors

Factor	sh HuR / sh ctrl
IGFBP4	0.38
Eotaxin 1 (CCL11)	0.55
VEGFR3 (FLT4)	1.48
ICAM2 (CD102)	1.75
ICAM3 (CD50)	1.96
RANTES (CCL5)	2.03
LIGHT (TNFSF14/CD258)	2.17
TIMP2	2.80
PDGF BB	3.58
CCL28	>>1

In a first validation step, I analyzed the mRNA expression of these factors in spheroids (Figure 6). While LIGHT and CCL11 mRNA could not be detected at all, ICAM3, VEGFR3, ICAM2, PDGF BB, and TIMP2 were not altered between sh HuR and sh ctrl spheroid. The latter observation does not exclude a potential translational regulation of certain targets by HuR. In contrast, CCL5, CCL28, and IGFBP4 displayed a similar behavior at mRNA and at protein level.

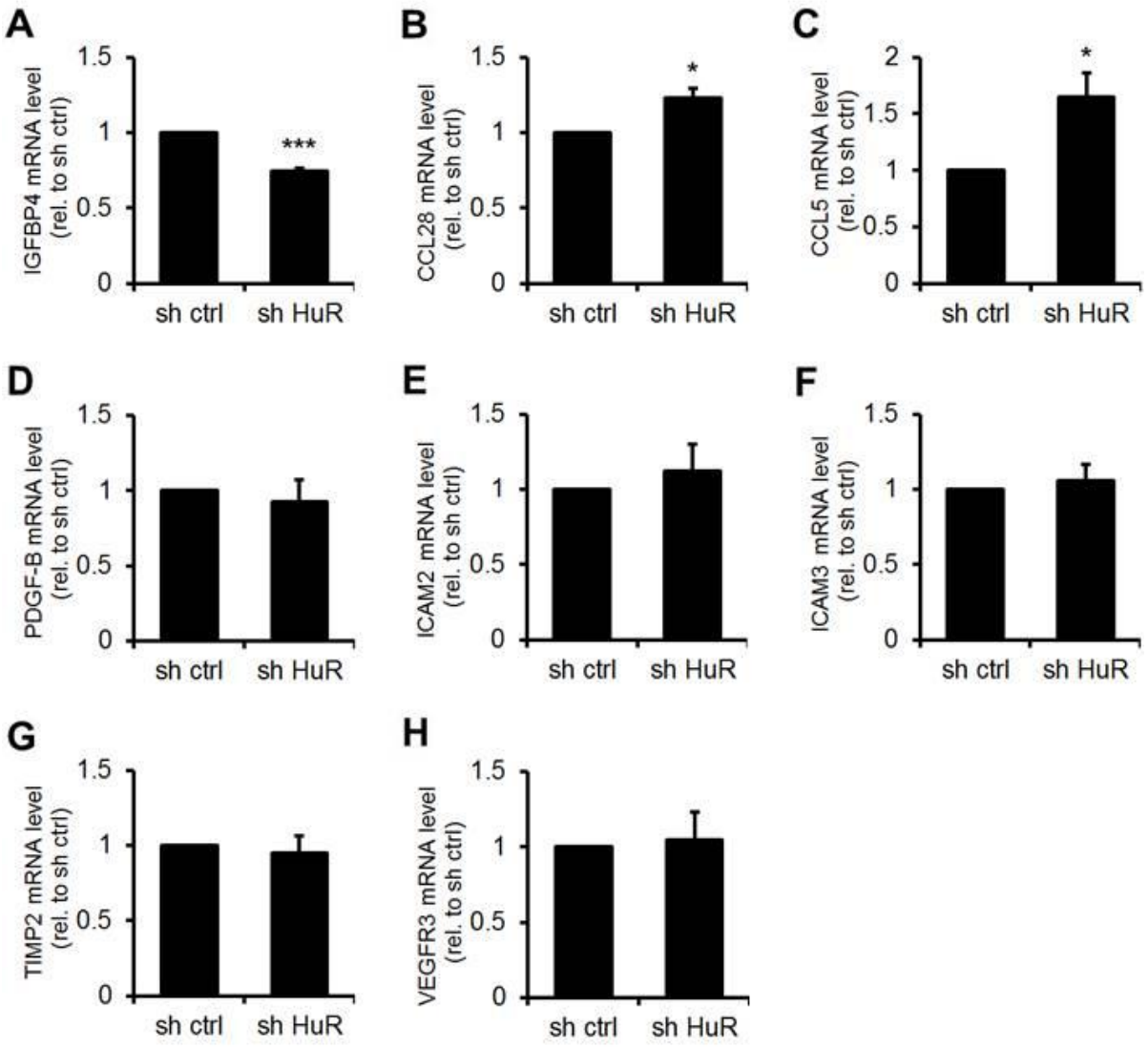

Figure 6: mRNA levels of selected targets in sh ctrl and sh HuR spheroids
Spheroids of sh ctrl and sh HuR cells were harvested after 7 days. mRNA expression of **(A)** IGFBP4, **(B)** CCL28, **(C)** CCL5, **(D)** PDGF-B, **(E)** ICAM2, **(F)** ICAM3, **(G)** TIMP2 and **(H)** VEGFR3 was analyzed by qPCR and normalized to actin and nucleolin mRNA levels. Data represent means ± SEM ($n \geq 3$; $^{*}p < 0.05$, $^{***}p < 0.001$).

To assess if the regulation of the three candidate HuR target mRNAs is selective for the complex spheroid setting, I additionally measured the mRNA expression of CCL28, CCL5, and IGFBP4 in monolayer cells. In line with the observations in the 3D culture, CCL28 and CCL5 mRNA expression was elevated in sh HuR as compared to sh ctrl monolayer MCF-7 cells. In contrast, the regulation of IGFBP4 appeared to be limited to the spheroids (Figure 7).

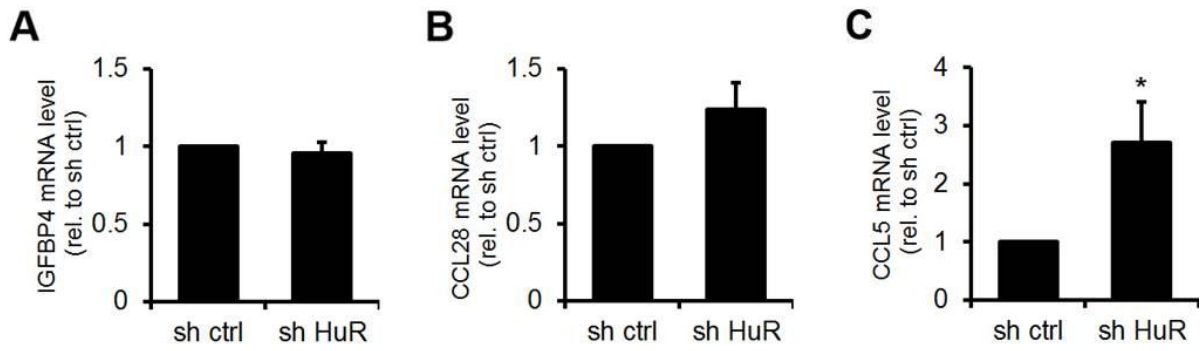

Figure 7: mRNA levels of selected targets in monolayer cells
sh ctrl and sh HuR cells were grown as monolayer cultures. IGFBP4 **(A)**, CCL28 **(B)**, and CCL5 **(C)** mRNA expression was analyzed by qPCR and normalized to actin and nucleolin mRNA levels. Data represent means ± SEM ($n \geq 3$; $^*p < 0.05$).

Among the analyzed targets, CCL5 did not only show the strongest effect in response to HuR depletion, it also appears as a novel, not yet described target of HuR. Moreover, CCL5 secretion by breast cancer cells is considered a determinant for the recruitment of leukocytes to the tumor site. As the mechanisms by which HuR negatively regulates target mRNAs are not well understood so far, I aimed at characterizing the mechanistic aspects of this regulation.

Taken together, in the context of 3D tumor spheroid MCF-7 cultures, HuR appears to primarily limit the expression of various cytokines and chemokines. Moreover, whereas the majority of putative targets is not regulated at mRNA expression, CCL28 and CCL5 showed consistent increases on protein and mRNA level in HuR knockdown spheroids as well as in 2D cultures.

4.2 Mechanism of HuR-dependent CCL5 regulation

Amongst the candidates CCL5 displayed the strongest and most consistent HuR-dependent phenotype, yet it was not described as a HuR target before. As CCL5 secretion by breast cancer cells is considered a determinant for the recruitment of leukocytes to the tumor site, I decided to focus my investigations on the characterization of the mechanism of HuR-mediated repression of CCL5 and its impact on the tumor-immune cell interactions within the tumor microenvironment.

4.2.1 HuR regulates CCL5 mRNA levels without affecting mRNA stability

As the regulation of CCL5 was not restricted to the spheroid setup, I used monolayer cells for the following mechanistic studies. In a first experiment, I analyzed the CCL5 mRNA results in a second knockdown clone, validating that both clones showed a similar upregulation of CCL5 mRNA (Figure 8A), in line with the comparable knockdown efficiencies of HuR (Figure 1). To test, if the changes in CCL5 expression translate into an altered CCL5 profile in MCF-7 monolayer cells, I measured CCL5 protein abundance in the supernatants of MCF-7 monolayer cultures and observed a 4 fold higher concentration in supernatants of sh HuR cells as compared to sh ctrl supernatants (Figure 8B).

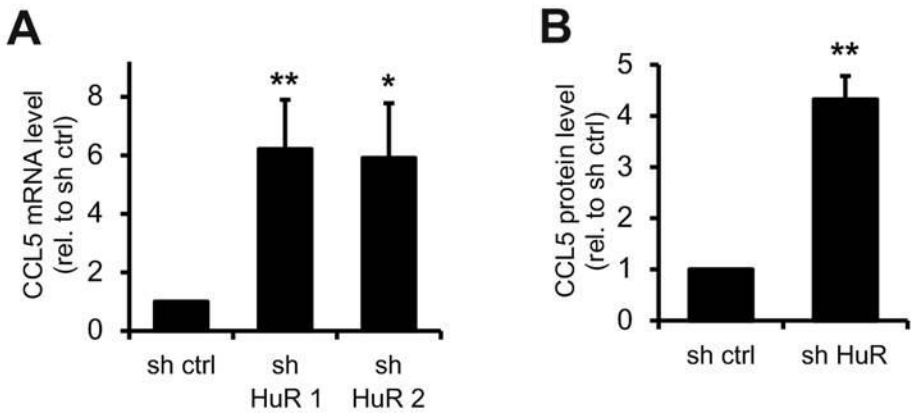

Figure 8: CCL5 levels in monolayer cells

(A) CCL5 mRNA expression in sh ctrl cells and two different sh HuR clones cells was analyzed by qPCR and normalized to actin and nucleolin mRNA levels. **(B)** CCL5 protein levels were analyzed in supernatants of sh ctrl and sh HuR MCF-7 cells by CBA analysis. Data represent means ± SEM ($n > 5$; $*p < 0.05$, $**p < 0.01$).

To assess if the observed regulation of CCL5 is specific to MCF-7 cells only, I depleted HuR in a panel of cancer cell lines from different origins and analyzed CCL5 mRNA expression. In fact, knocking down HuR in human lung carcinoma (A549), glioblastoma (T98G), and melanoma (A375) cells resulted in elevated CCL5 mRNA expression in all cases (Figure 9). Interestingly, while A549 lung carcinoma cells only showed a moderate depletion of HuR, the CCL5 increase was by far the strongest.

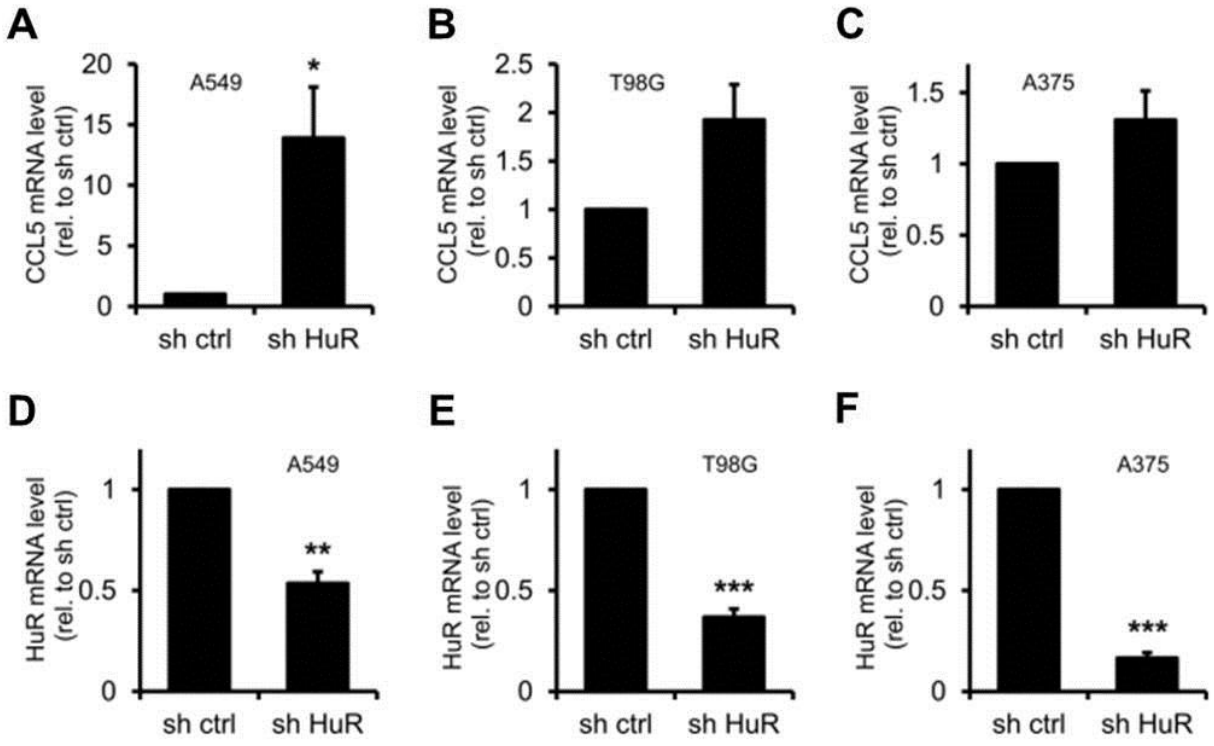

Figure 9: HuR-depletion enhances CCL5 expression in various tumor cell lines
(A-C) CCL5 and **(D-F)** HuR mRNA expression in sh ctrl and sh HuR **(A, D)** A549, **(B, E)** T98G and **(C, F)** A375 cells were analyzed by qPCR. mRNA levels were normalized to actin and nucleolin mRNA levels. Data represent means ± SEM ($n \geq 5$; *$p < 0.05$, **$p < 0.01$, ***$p < 0.001$).

Thus, the HuR-dependent repression of CCL5 expression is not restricted to MCF-7 cells and rather appears to constitute a unknown mode of CCL5 regulation not characterized so far.

HuR is generally considered as a post-transcriptional regulator, i.e. it mainly regulates mRNA decay and translation. As the HuR-dependent changes in CCL5 protein were in accordance with the mRNA changes, indicating that the regulatory mechanism should target the mRNA expression rather than the translation, I determined the stability of the CCL5 transcript after blocking *de novo* transcription with actinomycin D. While mRNAs with a high turn-over rate, i.e. transcripts that are subject to mRNA decay mechanisms, commonly have half-lives shorter than 8 hours, the CCL5 mRNA appeared to be extremely stable in MCF-7 cells, indicating that such mechanisms likely do not contribute to CCL5 regulation (Figure 10). In line, HuR knockdown cells exhibit similar kinetics, ruling out HuR-dependent changes in mRNA stability as the underlying principle of CCL5 regulation.

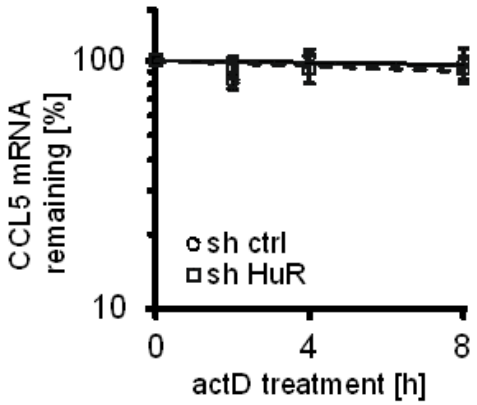

Figure 10: CCL5 mRNA stability is not affected by HuR depletion
CCL5 mRNA levels in MCF-7 cells were measured by qPCR at indicated points of time after blocking de novo transcription using actinomycin D (actD, 5 µg/mL). mRNA levels were normalized to actin and nucleolin mRNA levels. Data represent means ± SEM (n > 5).

Taken together, my results indicate that while HuR is generally considered to regulate the expression of its targets by affecting either the stability or the translation of the respective target mRNAs, it represses CCL5 mRNA and protein expression not in a post-transcriptional manner.

4.2.2 HuR depletion causes transcriptional upregulation of CCL5

Having excluded post-transcriptional modes of regulation, I next questioned if HuR regulates CCL5 transcription. To address this question, I isolated the putative CCL5 promoter from genomic MCF-7 DNA and inserted it into a pGL3-basic vector backbone. This vector system allows for analyzing the transcriptional activity of promoter elements in a luciferase-based reporter assay. Strikingly, CCL5 promoter activity was 3 fold induced in HuR depleted cells as compared to sh ctrl cells (Figure 11).

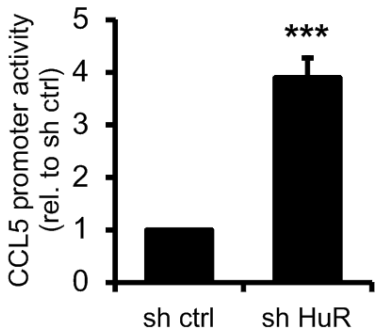

Figure 11: HuR depletion enhances CCL5 promoter activity
pGL3-basic vector containing the CCL5 core promoter (-812 to -1 relative to the transcription start side) was co-transfected with pRL-SV40 into MCF-7 cells. *Firefly* luciferase activity was normalized to *renilla* luciferase activity. Data represent means ± SEM (n ≥ 5; *p < 0.05, **p < 0.01, ***p < 0.001).

Thus, in contrast to its well-established role as a post-transcriptional regulator, HuR controls CCL5 expression on a transcriptional level.

4.2.3 Identification of the decisive promoter region

The CCL5 core promoter was identified and characterized in previous studies [35]. To further narrow down the relevant promoter region, I generated smaller fragments of the core promoter by successively removing parts from the 5' end. These constructs were then tested in MCF-7 cells wildtype or deficient of HuR. Interestingly, shortening the core promoter region from the initial 812 to only 140 nucleotides only marginally reduced the increase observed in sh HuR cells (Figure 12). In fact, only the vector containing the last 90 nucleotides did not show the upregulation in response to a HuR knockdown.

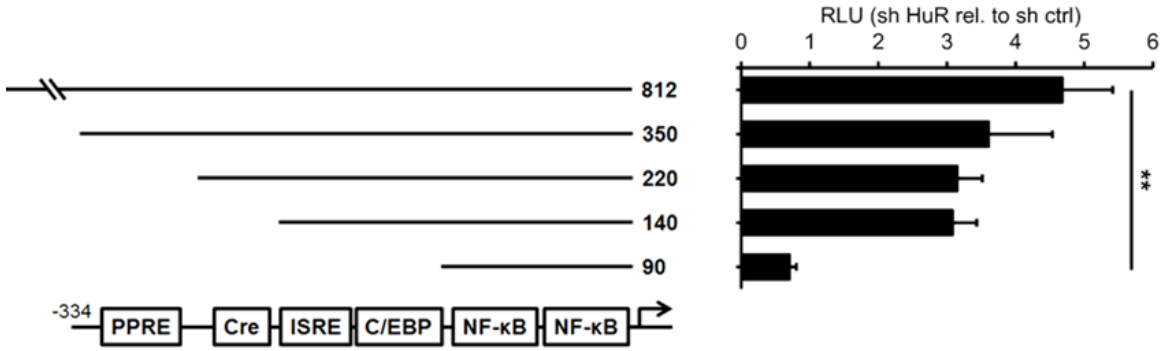

Figure 12: Transcriptional regulation by HuR depends on a defined promoter region

pGL3 basic vector containing different fragments of the CCL5 core promoter (from indicated positions to -1 relative to the transcription start side) was co-transfected with pRL-SV40 into MCF-7 cells. Firefly luciferase activity was normalized to renilla luciferase activity. Data represent means ± SEM (n ≥ 5; **p < 0.01).

These data indicate that the region in the promoter lying between 140 and 90 nucleotides upstream of the transcriptional start site is responsible for the transcriptional repression of CCL5 by HuR.

4.2.4 HuR regulates ISRE-associated signaling

The promoter region identified to mediate the HuR effect on CCL5 transcription contains two experimentally validated transcription factor binding sites directly adjacent to each other, an interferon stimulated response element (ISRE) and a C/EBP response element [34]. To address each element separately, I specifically deleted the respective transcription factor binding sites in the full size construct. Knowing that transcriptional activation of CCL5 by these sites may additionally involve cooperative binding of NF-κB, I also generated a promoter construct lacking the downstream NF-κB binding sites

(-71 to -40 relative to the transcription start site). Strikingly, while deleting the C/EBP and NF-κB sites had only very little influence on the HuR dependent increase of the CCL promoter activity, this effect was completely abrogated in the ISRE deletion construct (Figure 13). As a side note, the ISRE as well as the NF-κB sites appeared to be critical determinants for basal CCL5 transcription as their deletion reduced the activity in sh ctrl cells as well.

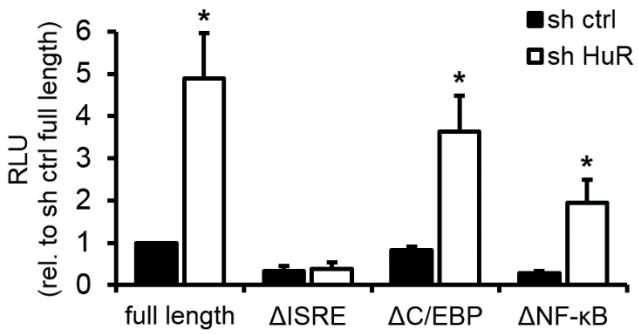

Figure 13: CCL5 regulation by HuR depends on an ISRE
pGL3-basic vector containing the indicated CCL5 promoter deletion constructs was co-transfected with pRL-SV40 into MCF-7 cells. *Firefly* luciferase activity was normalized to *renilla* luciferase activity. Data represent means ± SEM ($n \geq 5$; $^*p < 0.05$).

In summary, these data implicate that the elevated CCL5 levels in HuR knockdown cells likely result from increased promoter activity mediated by the ISRE within the CCL5 promoter.

4.2.5 CCL5 upregulation is independent of IFNβ downstream signaling

The finding that depletion of HuR suffices to provoke increased ISRE signaling was surprising given the fact that the ISRE within the CCL5 promoter is typically linked to CCL5 induction by inflammatory stimuli, most notably interferons (already indicated by the term ISRE as an acronym for interferon stimulated response element) [73].
I therefore speculated that interferon signaling might be involved in my system. To address this question, I first examined the expression of IFNα, IFNβ, and IFNγ in dependence of the HuR status of the cells. While IFNα and IFNγ mRNAs were neither detectable in sh ctrl nor in sh HuR cells, IFNβ mRNA levels could be measured in both cell lines and were significantly upregulated in HuR knockdown cells (Figure 14).

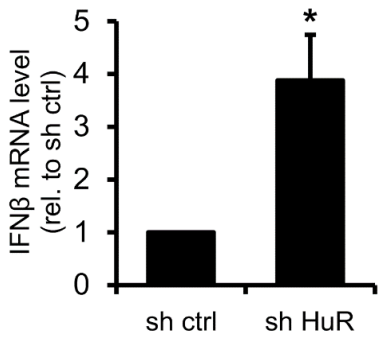

Figure 14: IFNβ is upregulated in HuR kd cells
IFNβ mRNA levels in sh ctrl and sh HuR MCF-7 cells were analyzed by qPCR and normalized to actin and nucleolin mRNA levels. Data represent means ± SEM ($n > 5$; $*p < 0.05$).

As CCL5 and IFNβ expression nicely correlated, I next asked if CCL5 regulation is a consequence of altered IFNβ levels. As IFNβ dependent regulation of CCL5 mandatorily requires activation of the respective IFNβ receptor IFNAR, first aimed at inhibiting IFNβ signaling using a neutralizing antibody against the IFNAR receptor. Yet, blocking the IFNβ receptor in HuR knockdown cells had no effect on CCL5 expression (Figure 15A). To further address the role of secreted IFNβ, i.e. paracrine signaling, in this setting, I used a transwell co-culture of sh ctrl cells in the lower compartment together with either sh ctrl or HuR knockdown cells in the upper compartment and determined changes in the sh ctrl cells in the lower compartment. Yet, the presence of HuR knockdown cells did not increase CCL5 levels in sh ctrl cells (Figure 15B).

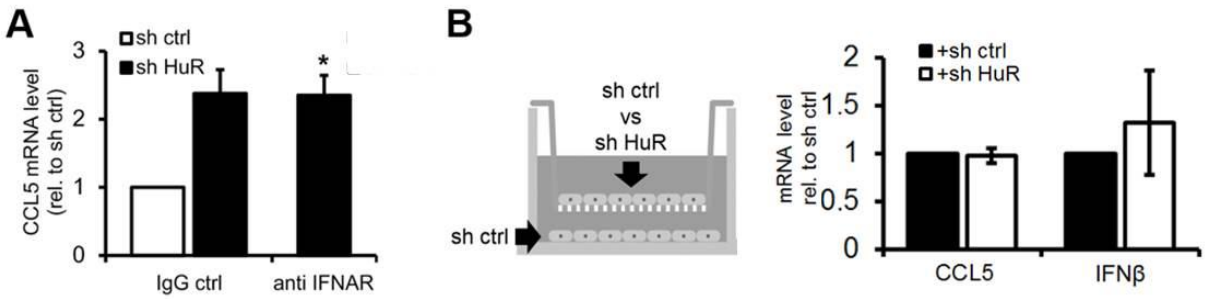

Figure 15: IFNβ does not affect HuR dependent CCL5 regulation
(A) Sh ctrl and sh HuR MCF-7 cells were cultured in the presence of a neutralizing antibody against the type I interferon receptor (αIFNAR, 10 µg/mL) or an isotype control IgG (IgG ctrl, 10 µg/mL) for 48 h. CCL5 mRNA expression was analyzed by qPCR and normalized to actin and nucleolin mRNA levels. **(B)** Transwell co-culture of sh ctrl and sh HuR cells. sh ctrl cells (bottom) were co-cultured with either sh ctrl or sh HuR cells (transwell insert, pore size: 0.4 µm) as illustrated by the schematic diagram. After 48 h, mRNA was isolated from the sh ctrl cells in the lower compartment and analyzed for CCL5 and IFNβ expression. All mRNA levels were normalized to actin and nucleolin mRNA levels. Data represent means ± SEM (n ≥ 3; *p < 0.05).

These data suggest that despite the proven importance of the ISRE in the CCL5 promoter and the elevated expression of IFNβ in HuR depleted cells, IFNβ does not contribute to the HuR-dependent repression of CCL5 in MCF-7 cells.

4.2.6 IRF expression in MCF-7 cells

After ruling out interferons, I hypothesized that a distinct and clearly defined mechanism rather than a general ISRE activation might underlie the observed CCL5 regulation in my experimental setup. In general, ISREs are recognized by the 9 members of the interferon regulatory factor (IRF) family. Therefore, I next analyzed the mRNA expression of the IRFs. Yet, since IRF4, IRF6, and IRF7 are described as immune cell specific [74, 75] and IRF8 was not detectable, these were excluded from the analysis. Of the tested IRFs, only IRF1 and IRF9 were upregulated in sh HuR cells, while all other IRFs were not significantly altered (Figure 16).

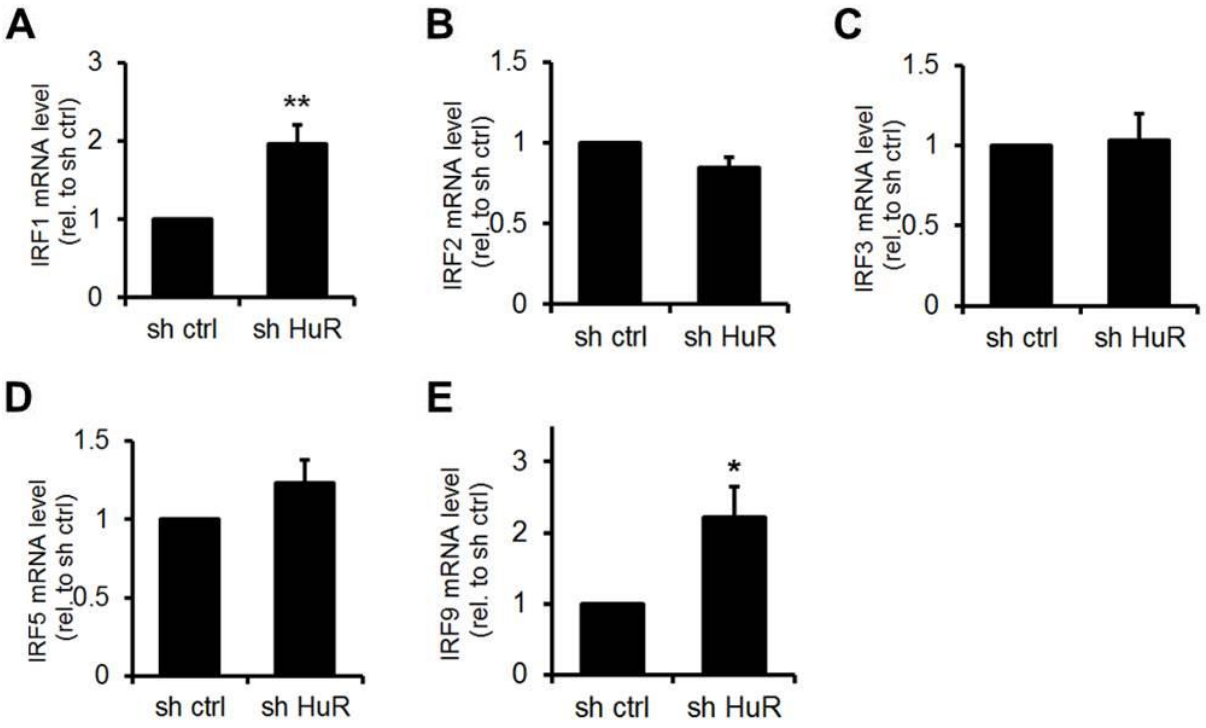

Figure 16: mRNA expression of IRFs in HuR kd cells
mRNA expression of **(A)** IRF1, **(B)** IRF2, **(C)** IRF3, **(D)** IRF5, and **(E)** IRF9 in sh ctrl and sh HuR MCF-7 cells was analyzed by qPCR and normalized to actin and nucleolin mRNA levels. Data represent means ± SEM ($n \geq 3$; $^*p < 0.05$, $^{**}p < 0.01$).

Therefore, IRF 1 and 9 emerged as interesting candidates for further investigations. Nevertheless, since IRF3 and 5 are commonly regulated via post-translational modifications affecting their transcription factor activity rather than by mRNA expression changes, these candidates were also considered.

4.2.7 Subcellular localization and activation state of selected IRFs

Under basal conditions, IRF3 is inactive, while activation stimuli lead to phosphorylation and hence activation of IRF3 [76]. Therefore, I tested the phosphorylation status of IRF3 in sh ctrl and sh HuR cells. Phosphorylated IRF3 could neither be detected under basal nor under HuR depleted conditions (Fig. 5.17). To verify that IRF3 is indeed phosphorylated upon activation in my system, I further tested IRF3 phosphorylation in cells transfected with a plasmid (pGL3) or stimulated with poly(I:C) as exogenous nucleic acids have been shown to activate IRF3 [77]. While poly(I:C) strongly induced phosphorylation of IRF3 irrespective of the HuR status, plasmid DNA had not effect (Figure 17 *lanes 3-6*).

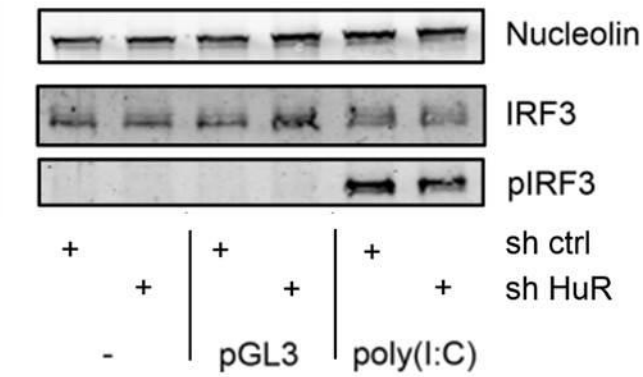

Figure 17: IRF3 is not activated in sh HuR cells
sh ctrl and sh HuR MCF-7 cells were left untreated, transfected with a pGL3-vector, or transfected with poly(I:C) (2 µg/mL) and harvested after 24h. Protein levels of IRF3 and pIRF3 were analyzed by Western blot analysis. Poly(I:C) served as a positive control, Nucleolin served as a loading control. Blot is representative for three independent experiments.

As these findings excluded IRF3 as responsible mediator, I next analyzed protein levels of IRF1, IRF5, and IRF9 in whole cell lysates as well as in the nuclear fractions. β-Tubulin and H3 served as controls for the purity of the subcellular fractionation. While IRF5 remained unaltered in whole cell and nuclear lysates, both IRF1 and IRF9 showed elevated expression in HuR knockdown cells (Figure 18). Interestingly, only IRF9 also showed increased presence in the nuclear fraction as well.

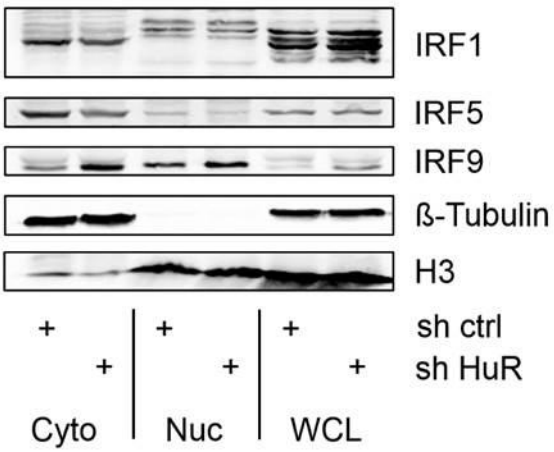

Figure 18: Expression and subcellular fractionation of IRFs in HuR kd cells
Protein levels of IRF1, IRF5, and IRF9 were analyzed in cytoplasmic (Cyto), nuclear (Nuc), or whole cell (WCL) lysates of sh ctrl and sh HuR MCF-7 cells by Western blot analysis. β-Tubulin and H3 served as loading controls. Blot is representative for three independent experiments.

As the elevated levels and nuclear accumulation of IRF9 in HuR depleted cells suggested a functional link to the increased CCL5 transcription, I next determined the nuclear levels of the obligatory transcriptional co-factor of IRF9, Stat1. Stat1 could be detected in the cytoplasm of sh ctrl and sh HuR cells, however, under both conditions no nuclear Stat1 could be detected (Figure 19).

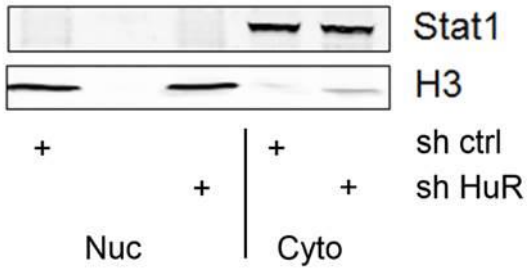

Figure 19: Stat1 is not present in the nucleus
Protein levels of Stat1 were analyzed in cytoplasmic (Cyto) and nuclear (Nuc) lysates of sh ctrl and sh HuR MCF-7 cells by Western analysis. H3 served as a loading control. Blot is representative for three independent experiments.

This result strongly suggested that IRF9 does not contribute to CCL5 transcription in this cellular system.

Having ruled out all other IRFs, I decided to revisit IRF1. Specifically, I aimed to analyze if elevated IRF1 protein, despite its little presence in the nucleus, might still contribute to the CCL5 regulation via binding to the CCL5 promoter. Therefore, I performed a ChIP analysis for IRF1. Yet, while IRF1 bound to the CCL5 promoter in sh ctrl cells, this association was lost in HuR knockdown cells (Figure 20).

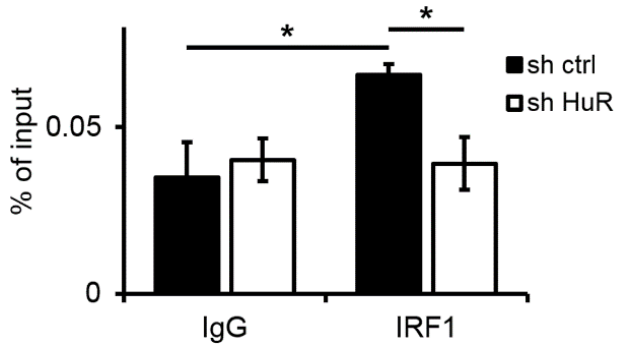

Figure 20: ChIP analysis of IRF1
Chromatin was co-immunoprecipitated out of sh ctrl and sh HuR cellular lysates using an antibody against IRF1 or an IgG isotype control antibody. Enrichment of the CCL5 promoter was analyzed by qPCR and normalized to input DNA levels. Data represent means ± SEM (n = 4; *p < 0.05).

As IRF1 is supposed to induce CCL5 transcription, this result finally excluded IRF1 and its functionally associated factors as the mediators of the HuR-dependent effect on CCL5 as well.

Taken together, while the CCL5 repression by HuR appears to be mediated by the ISRE in the promoter of CCL5, all my data argue against the involvement of canonical IRF-signaling in this process.

4.3 Role of HuR in MΦ recruitment

Having established that HuR depletion enhances CCL5 expression, which is a well-characterized chemokine, I next aimed to study the functional consequences of the HuR associated CCL5 regulation in the context of MΦ recruitment to the tumor site.

4.3.1 HuR affects MΦ recruitment into spheroids

To assess the interaction between tumor cells and MΦ, I first evaluated MΦ recruitment into MCF-7 tumor spheroids. Therefore, I isolated primary MOs from human blood samples and applied them to 5 days old spheroids. To study the kinetics of infiltration, I analyzed the presence of $CD14^+$ cells, i.e. MΦ, within the spheroids after 2 and 5 days of co-culture. In fact, similarly elevated MΦ infiltration into HuR deficient spheroids was observed after 2 and 5 days (Figure 21). While the increase was slightly higher at day 5, these data suggested that the impact of HuR on the infiltration of MΦ manifests early during the co-cultures already.

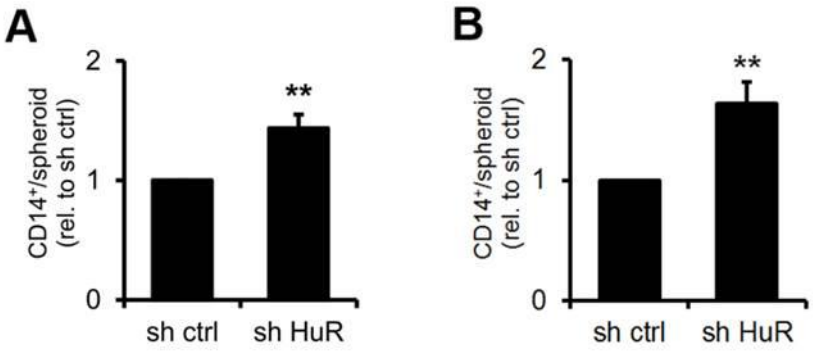

Figure 21: MΦ recruitment into HuR-kd MCF-7 tumor spheroids
MCF-7 spheroids were co-cultured with primary human MOs for (A) 2 or (B) 5 days. MΦ infiltration was analyzed by flow cytometry using an antibody against CD14. Data represent means ± SEM ($n \geq 5$; $^{**}p < 0.01$).

To minimize potential secondary effects, I decided to use 2 day infiltrations in further experiments.

To test, if the elevated MΦ contents in HuR knockdown spheroids were due to changes in the viability or proliferation of the MΦ, I examined proliferation by staining of the proliferation marker Ki-67 and apoptosis by staining cleaved, i.e. active, caspase 3. As expected, MΦs did not proliferate at all in this setting, i.e. no KI-67 positive MΦs were detectable (Figure 22). Furthermore, the amount of apoptotic MΦs remained unaltered in sh HuR spheroids as compared to sh ctrl spheroids, indicating that tumor HuR levels did not affect the viability of the infiltrating MΦ.

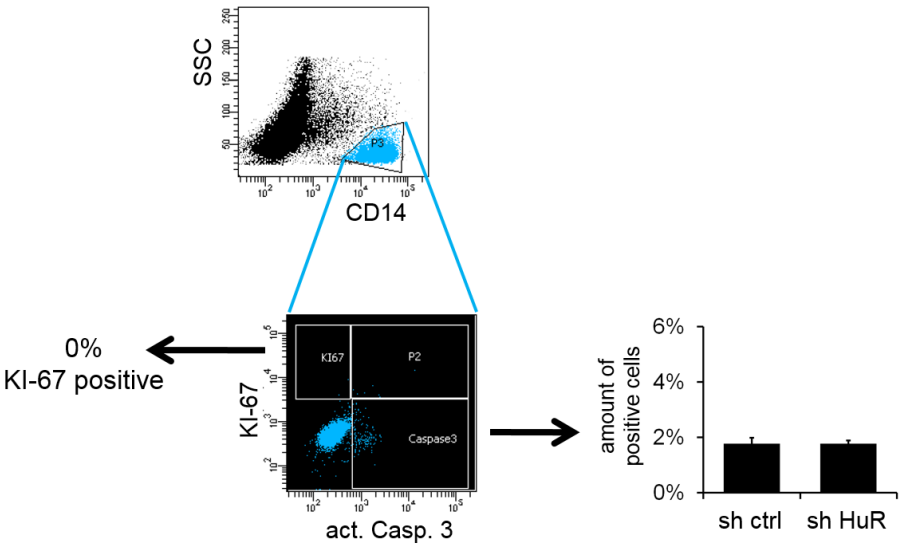

Figure 22: Apoptosis and proliferation of spheroid-recruited MΦs
MCF-7 spheroids were co-cultured with primary human MOs for 2 days. MΦs were identified by flow cytometry using an antibody against CD14 and stained for KI-67 and active caspase 3. Data represent means ± SEM (n = 2).

Thus, my results indicate that HuR expression in tumor cells does not affect MΦ proliferation or viability, but attenuates the infiltration of MΦ potentially by altering the recruitment process.

4.3.2 MO migration towards spheroid supernatants

As CCL5 is an important chemoattractant, I next aimed at determining the chemoattractive properties of sh ctrl vs. sh HuR spheroids on freshly isolated primary MOs. To this end, I cultured primary MOs in the upper chamber of a Boyden chamber assay providing supernatants of the tumor spheroids in the lower compartment as a

chemoattractant. Surprisingly, no differences could be observed between the migration of MOs towards sh ctrl or sh HuR supernatants (Figure 23A). To assess if an initial contact between MOs and tumor cells is needed to provoke the signals inducing the enhanced the infiltration of the MΦs into the HuR kd spheroids, I next used supernatants of spheroid-MΦ co-cultures as chemoattractant for MOs. Yet, again the supernatants of spheroid-MΦ co-cultures failed to induce a differential migratory response (Figure 23B).

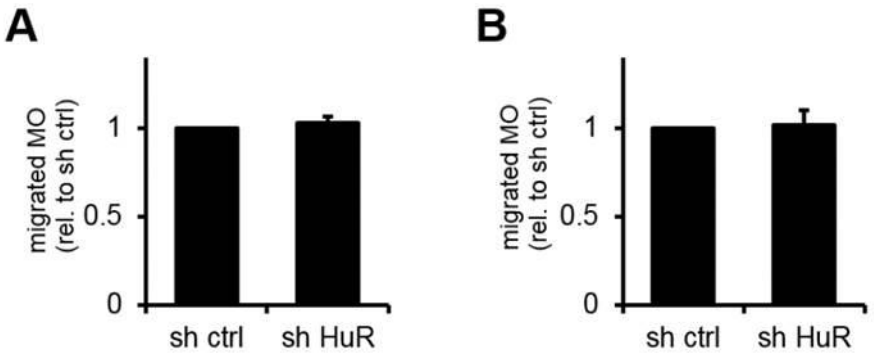

Figure 23: MO migration towards spheroid supernatants
Chemotaxis of primary human MOs towards **(A)** spheroid or **(B)** co-culture supernatants was evaluated in a Boyden chamber. Migrated MOs were quantified by cell counting. Data represent means ± SEM (n ≥ 4).

Thus, while tumor cell HuR appears to limit the infiltration of MΦs into tumor spheroids, it does not affect the chemoattractive response of MOs, at least in a cell-free context.

4.3.3 Enhanced MΦ recruitment in HuR-deficient MCF-7 tumor spheroids is mediated by CCL5

Having ruled out changes in MΦ proliferation and viability as well as in the chemoattractive properties of spheroid supernatants depending on the tumor cell HuR status, yet considering the elevated presence of MΦs in HuR depleted spheroids, I next aimed to assess if CCL5 might directly contribute to the latter phenotype. In line with the cytokine array, HuR knockdown spheroids exhibited increased CCL5 protein levels (Figure 24A). To determine if these altered CCL5 levels affect MΦ recruitment into the spheroids, I used a neutralizing antibody against CCL5 and analyzed MΦ infiltration into sh ctr and sh HuR spheroids. In contrast to the migration assays (Figure 23), blocking CCL5 abrogated the HuR dependent increase in MΦ infiltration into the spheroids (Figure 24B).

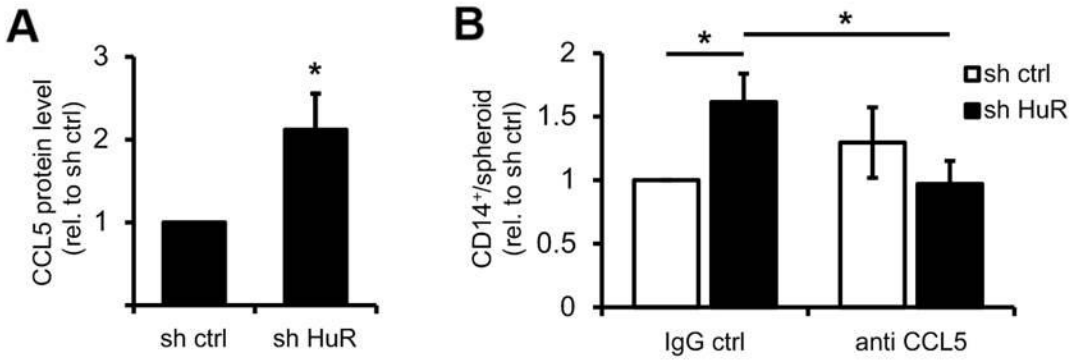

Figure 24: HuR knockdown in MCF-7 spheroids leads to increased, CCL5-mediated MΦ recruitment

(A) CCL5 protein levels in lysates of seven days old spheroids were measured by flow cytometry using a Cytometric Bead Array (CBA). **(B)** MCF-7 spheroids were co-cultured with primary human MOs for 2 days in the presence of a neutralizing CCL5 antibody (3 µg/mL) or an isotype control IgG (3 µg/mL). MΦ infiltration was analyzed by flow cytometry using an antibody against CD14. Data represent means ± SEM (n ≥ 5; *p < 0.05).

Strikingly, while CCL5 neutralization completely diminished MΦ recruitment into HuR knockdown spheroids, infiltration into sh ctrl spheroids remained entirely unaffected, supporting the notion that CCL5-induced infiltration is specific to HuR kd conditions in my experimental setting.

Taken together, these data suggest that a loss of HuR in MCF-7 spheroids upregulates CCL5, which in turn enhances MΦ recruitment into these spheroids.

4.3.4 *In silico* analysis in breast cancer tumor samples

Having established that the HuR-dependent repression of CCL5 in tumor cells accounts for an altered MΦ recruitment into tumor spheroids *in vitro*, I finally asked if this observation might hold true in breast tumor patients as well. To evaluate the impact of HuR on CCL5 expression and MΦ presence in primary tumors, I evaluated potential correlations between HuR, CCL5, and a MΦ signature (CD68, CD163, MSR1) in a cohort of ER-positive breast tumors (n = 404) within the TCGA database. Corroborating the *in vitro* findings, HuR showed a slight negative correlation with CCL5 (Figure 25A). Furthermore, HuR negatively correlated with the MΦ markers (CD68, CD163, MSR1) (Figure 25B). As expected, a strong positive correlation between CCL5 and the MΦ signature was observed (Figure 25C).

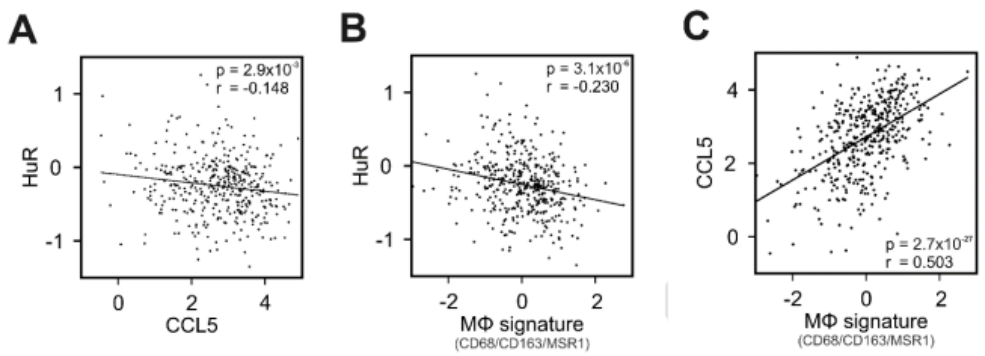

Figure 25: HuR expression in invasive breast carcinoma negatively correlates with CCL5 expression and MΦ presence

A cohort of ER-positive breast tumors (n=404) was analyzed for correlations between **(A)** HuR and CCL5, **(B)** HuR and MΦ markers CD68, CD163, and MSR1, and **(C)** CCL5 and the same MΦ signature. Statistical analysis was performed by Dr. Kristoffer von Stedingk (Lund University, Sweden). Data are presented as scatter plots of mean log2 normalized expression values (HuR and CCL5) and z-score based MΦ signatures for individual tumors. Pearson's correlation coefficient and p-values are included.

Thus, while high CCL5 expression in breast tumors is predictive for enhanced MΦ infiltration, elevated HuR expression in tumors appears to be negatively associated with both CCL5 expression and concomitant MΦ recruitment.

In summary, I identified CCL5 as a novel HuR-repressed target in tumor cells. Mechanistically, HuR appears to inhibit ISRE-dependent transcription of CCL5. As a consequence of its CCL5 inhibitory effect, HuR also also limits MΦ recruitment into 3D tumor spheroids *in vitro*. In line, HuR expression in breast tumor patient samples negatively correlates with both CCL5 levels and MΦ infiltration.

5 Discussion

Elevated HuR expression or activity has been correlated with malignant progression in a broad variety of different cancer types. While HuR was functionally linked to increased proliferation, apoptosis resistance, angiogenesis, and metastasis in various tumor cell line models, its potential to regulate inflammatory processes in the tumor microenvironment has been rarely addressed so far.

Thus, in the present work I aimed to determine the impact of HuR in tumor cells on their interplay/-action with immune cells, specifically MOs/MΦs. Initially, I identified the chemokine CCL5 as a novel HuR target in MCF-7 cells frown in 2D and 3D cultures. I further characterized the HuR-dependent regulation of CCL5 as transcriptional repression mediated via an ISRE element within the CCL5 promoter. Importantly, elevated expression of CCL5 in HuR-deficient tumor cells sufficed to enhance the recruitment of MΦs into 3D tumor spheroids. Interestingly, the negative correlation between HuR and CCL5 but also a MΦ signature in tumors also holds true for primary invasive breast tumors.

5.1 Mechanistic considerations of the HuR-CCL5 axis

The fact that CCL5 mRNA expression was increased in HuR-depleted cells was rather surprising considering that HuR predominantly exerts positive regulatory post-transcriptional functions, i.e. HuR for the most part stabilizes target mRNAs and enhances translation of target mRNAs. However, mRNA destabilization by HuR was occasionally observed and might require cooperative binding with further destabilizing factors like AUF1 or KSRP, as reported for c-myc, npm1, and p16 [60, 78]. Moreover, to my knowledge, this study is the first to provide direct evidence for a HuR-dependent transcriptional regulation of inflammatory mediators. There have been previous reports though, which provided indications for HuR acting on a transcriptional level to regulate cytokine expression remains to be finally proven. Yiakouvaki et al. observed elevated mRNA levels of IL6, IL12, and CCL7 in HuR-ko MΦ,excluding a post-transcriptional mechanism [79]. Furthermore, it has been previously observed that HuR may regulate mRNA expression of VEGF, CCL2, and CCL8 without affecting their mRNA stability [69, 80]. The underlying mechanisms were not addressed, though. Further evidence for a transcription regulatory function of HuR were provided by Katsanou et al., who found that HuR may simultaneously

regulate transcription, mRNA stability, and translation of inflammatory factors like TNFα and CCL2 [81]. My data on the other hand indicate that the HuR-mediated repression of CCL5 is exclusively mediated by a transcriptional mechanism, in fact CCL5 appeared to be intrinsically very stable in MCF-7 cells ($t_{½}$>>8h), which again speaks against the involvement of any mRNA decay mechanisms. Corroborating this notion, *in silico* analysis using the ARESite database [82] predicted no direct interaction between AUBPs and CCL5. In contrast to my results, several groups reported much shorter mRNA half-lives and secondary stabilization following transcriptional upregulation of CCL5 in benign tissue [83-86], however the regulatory *cis*-elements and respective *trans*-acting factors are still unknown. A recent study identified a GU-rich element (GRE) in the CCL5 3'UTR bound by the destabilizing RBP CELF1 [87]. Interestingly, CELF1 is typically downregulated in response to cytokine activation and appears to be permanently inactive in cancer cells [88]. Therefore, one might speculate that permanent silencing of destabilizing factors like CELF1 in the course of malignant transformation plays a key role in maintaining robust expression of CCL5 in cancer cells.

Promoter activity of CCL5 has been mainly attributed to the proximal genomic region with the core promoter spanning from -220 to +1 being sufficient for full transcriptional activation under most conditions [34, 89]. This core promoter contains two adjacent NF-κB binding sites, an interferon-stimulated response element (ISRE), a C/EBP binding motif, and a cAMP response element (CRE). Furthermore, a distal PPARγ response element was postulated based on reporter assays with PPARγ modulators [36, 90], however so far without further indications for a functional relevance. In addition, a frequent single nucleotide polymorphism at position -401 was reported to produce a functional GATA binding site and is suggested to correlate with the risk of several cancers, including breast cancer. Nevertheless, constitutive expression of CCL5 in cancer cells was predominantly attributed to increased NF-κB activity, however also elevated JNK and MAPK signaling, leading to binding of c-Jun to the CRE, was reported to be crucial in this context. Furthermore, it was shown that prolonged Stat3 signaling can lead to CCL5 activation by an unconventional NF-κB complex consisting of unphosphorylated, i.e. usually inactive, p65/p50 and unphosphorylated Stat3 [42]. This mechanism was proposed to allow for prolonged CCL5 expression after TNFα stimulation, caused by the TNFα-dependent induction of IL6 which maintains Stat3 activation by an autocrine feedback loop. In my

experiments, deletion of the NF-κB binding sites strongly reduced CCL5 promoter activity in a HuR-independent manner only. Therefore, I assumed that NF-κB is required for basal expression of CCL5. Strikingly, the increase in promoter activity in HuR-depleted cells was completely abrogated by ISRE deletion while it remained constant among all other constructs. ISREs are bound by members of the IRF transcription factor family. Corroborating the involvement of IRFs, similar effects were seen when specifically mutating 6 nucleotides in the core IRF binding site (data not shown). The ISRE-associated promoter activity in wildtype cells raised the question which IRFs contribute to basal CCL5 expression and how this pattern changes in response to HuR-depletion.

Little is known about the role of IRFs in constitutive CCL5 expression. Studies about ISRE-mediated upregulation of CCL5 are typically based on prestimulation with viral particles or proinflammatory factors. While all tumor-associated IRFs respond to distinct inflammatory stimuli, pronounced activity under basal conditions appears to be restricted to IRF1, its competitive repressor IRF2, and, to a lesser extent, IRF5 [74, 75]. In line, I could demonstrate that IRF1 binds to the CCL5 promoter in wildtype MCF-7 cells. Surprisingly, this association was lost in HuR-kd cells, contradicting the general increase in ISRE-associated transcription. However, while HuR-depletion slightly increased IRF1 mRNA expression it did not affect nuclear levels of IRF1 protein, suggesting another level of interference. With regards to the functional outcome, an inhibitory binding of IRF2 might be considered as an underlying mechanism. Yet, my results clearly rule out the involvement of IRF1 in the enhanced CCL5 transcription in HuR-kd cells altogether, implying the presence of a different factor, which is not a repressor like IRF2. In that context, the decreased promoter binding of IRF1 might rather be the result of a competitive displacement by another transcriptional activator targeting the ISRE. In line with previous studies [91], I could detect a small pool of nuclear IRF5, while most of the protein was localized to the cytoplasm which reflects the basal, i.e. inactive state. This expression pattern remained unchanged under HuR-deprived conditions. Therefore, while I cannot exclude a functional role of IRF5 in basal CCL5 expression, it is unlikely to contribute to the HuR-dependent CCL5 expression changes as well. Supporting this notion, CCL5 was also induced in HuR-depleted MDA-MB-231 cells, which were repeatedly reported to lack IRF5 protein [92, 93]. My mRNA expression analyses further indicate that HuR-depletion induces the endogenous type I IFN (IFN1) signaling pathway.

Specifically, the concomitant upregulation of IRF1, IRF7, and IRF9 resembled a characteristic induction pattern in response to IFN1 activation, suggesting that HuR represses IFN1 signaling, rather than modulating basal IRF activity. Supporting this notion, IFNβ mRNA levels were increased in HuR-kd cells. Along these lines, induction of endogenous IFNβ has been described as a regulatory mechanism that sustains CCL5 expression in astrocytes [94]. However, my data argue against autocrine IFNβ having a pronounced direct effect on CCL5 as CCL5 expression was induced in wildtype cells when co-cultured with HuR-kd cells. Moreover, blocking the IFN1 receptor (IFNAR1) in HuR-depleted cells also did not prevent the enhanced CCL5 expression. While the observed IFNβ induction might not suffice to directly induce downstream signaling, it still supports the concept of an induction pattern specific for IFN1 signaling. In fact, activation of IFN1 signaling cascades by endogenous stimuli can induce both CCL5 and IFN. In that case, IFNβ is not required for CCL5 induction but rather amplifies the signal by establishing a feed forward loop. Similarly, IRF1 can appear as both, an upstream activator as well as a downstream target of IFN1 signaling. Furthermore, as it was previously shown that small exogenous RNAs, e.g. siRNAs, can directly trigger an interferon response independent of the actually targeted sequence, yet apparently dependent on the sequence of the introduced RNA [95], it was important to see that the effect of HuR-depletion on CCL5 expression was validated using 5 different shRNA sequences. Since the absence of phosphorylated IRF3, a classical hallmark of the contact with exogenous nucleotides, further argues against the involvement of RNA/DNA-sensing pattern recognition receptors in my setting, I concluded that the observed CCL5 regulation indeed is due to an HuR-regulated, specific mechanism. While I was able to rule out canonical IRF-mediated activation of the ISRE of the CCL5 promoter in HuR-depleted cells, the exact link between HuR and the altered type 1 interferon signaling resulting in CCL5 transcription changes remains to be identified. As CCL5 and other interferon-related genes were recently shown to be upregulated in response to DNA damage in breast cancer [96], and the DNA repair protein RAD51 was shown to be positively regulated by HuR in breast cancer cells [97], it is tempting to speculate that HuR could affect CCL5 transcription via altered DNA damage response mechanisms. This concept would also fit nicely with the observation that loss of the BRCA2/RAD51-dependent DNA damage response enhances ISRE-dependent transcription [98].

5.2 Functional consequences of the HuR-CCL5 axis

Tumor-associated inflammation, while not presented as a hallmark of cancer by Hanahan and Weinberg in 2000 [7], is now generally accepted as a key characteristic of the tumor microenvironment and was therefore included in the 2011 update of this paper [8]. Upregulation of CCL5 in breast tumors is closely linked to this process by supporting the recruitment of TAMs. Corroborating this concept, HuR-depleted MCF-7 tumor spheroids that expressed elevated levels of CCL5 contained more MΦs. Since *in situ* proliferation, as postulated for blood monocyte-derived TAMs by Tymoszuk et al [99], as well as differences in MΦ apoptosis could also be excluded, this pointed to an altered infiltration phenotype. However, MOs showed no differential migration towards spheroid supernatants, suggesting that depletion of HuR specifically promoted haptotactic invasion into the spheroid structure. Subsequent infiltration experiments in the presence of a neutralizing antibody revealed that the enhanced MΦ infiltration into HuR kd spheroids is exclusively mediated by CCL5. Corresponding to this result, treatment with a competitive CCL5 inhibitor was previously shown to reduce TAM recruitment in murine breast tumor allografts [31]. Interestingly, though, while CCL is considered to be a critical mediator of MΦ recruitment, infiltration into wildtype spheroids appeared to be entirely CCL5-independent, indicating that basal infiltration in my model was mainly mediated by other chemokines, such as CCL2 or IL8. Apart from the attraction of myeloid cells to the tumor site, CCL5 is also implicated in tumor cell spreading [100]. HuR on the other hand is mainly considered to promote such processes by upregulating factors like CXCR4, MMP9, and uPA. Considering emerging evidence that HuR might play an ambiguous role, not only for inflammatory processes as suggested in this study, but also in terms of tumor invasion and metastasis, it may be important to address a potential involvement of the HuR-CCL5 axis in that context as well. While depletion of HuR alone does not affect the invasive potential of monolayer MCF-7, it was recently shown that HuR in fact counteracts epithelial-to-mesenchymal transition (EMT) in MCF-7 mammospheres by repressing the transcription of CD133 [101]. In line, EMT in MCF-7 is closely linked to the enrichment of a highly invasive $CD44^{+}/CD24^{-}$ cancer stem cell-like subpopulation [102] and requires the downregulation of the transcription factors GATA3 and ERα, which are both stabilized by HuR in this cell line [103, 104]. Strikingly, Yan et al. found that the cancer stem cell-like subpopulation of MCF-7 cell cultures showed an enriched IFN response gene

signature and increased CCL5 expression [105]. CCL5 was further shown to mediate the aggressiveness of $CD133^+$ stem cell-like ovary tumor cells [106]. Therefore, one might speculate that HuR and CCL5 are part of an interconnected network regulating EMT and dedifferentiation, particularly in luminal, ER^+ breast tumors. Therefore, HuR might inhibit EMT in ER^+ tumors by suppressing transcriptional activation of effector molecules, while promoting invasion in ER^- tumors.

Corresponding to the direct association of HuR with multiple tumor-associated processes in cell culture and animal models, several clinical studies in breast cancer patients found HuR to be associated with tumor progression and poor prognosis [65, 107, 108]. In my system, the effect of HuR modulation on MΦ recruitment was strictly CCL5-mediated. *In vivo*, it remains to be seen if established breast cancer-associated HuR-targets like IL8, HIF1-α, VEGF, MMPs, or PDGF-C might compensate for the HuR-dependent repression of CCL5, when HuR is expressed. In contrast, when HuR is missing, elevated CCL5 from tumor cells could stimulate the secretion of some of the aforementioned factors, including IL8, CCL2, and VEGF which were shown to be CCL5 responsive in TAMs, to counterbalance the downregulation of these factors under HuR-deprived conditions. My *in silico* analyses were in line with the notion that, in breast cancer patients, HuR indeed negatively correlates with CCL5 expression and MΦ presence. Considering that HuR is mainly seen as a potential promoter of cancer-associated inflammation, it might be interesting to analyze HuR-dependent changes in the polarization profile of recruited TAMs *in vivo* in future studies.

6 References

1. Fortunato, A., et al., *Natural Selection in Cancer Biology: From Molecular Snowflakes to* Trait *Hallmarks.* Cold Spring Harb Perspect Med, 2017. **7**(2).
2. Aktipis, C.A. and R.M. Nesse, *Evolutionary foundations for cancer biology.* Evol Appl, 2013. **6**(1): p. 144-59.
3. Burnet, F.M., *The concept of immunological surveillance.* Prog Exp Tumor Res, 1970. **13**: p. 1-27.
4. Nowell, P.C., *The clonal evolution of tumor cell populations.* Science, 1976. **194**(4260): p. 23-8.
5. Merlo, L.M., et al., *Cancer as an evolutionary and ecological process.* Nat Rev Cancer, 2006. **6**(12): p. 924-35.
6. Beerenwinkel, N., et al., *Cancer evolution: mathematical models and computational inference.* Syst Biol, 2015. **64**(1): p. e1-25.
7. Hanahan, D. and R.A. Weinberg, *The hallmarks of cancer.* Cell, 2000. **100**(1): p. 57-70.
8. Hanahan, D. and R.A. Weinberg, *Hallmarks of cancer: the next generation.* Cell, 2011. **144**(5): p. 646-74.
9. Pietras, K. and A. Ostman, *Hallmarks of cancer: interactions with the tumor stroma.* Exp Cell Res, 2010. **316**(8): p. 1324-31.
10. Hanahan, D. and L.M. Coussens, *Accessories to the crime: functions of cells recruited to the tumor microenvironment.* Cancer Cell, 2012. **21**(3): p. 309-22.
11. Schito, L., *Bridging angiogenesis and immune evasion in the hypoxic tumor microenvironment.* Am J Physiol Regul Integr Comp Physiol, 2018. **315**(6): p. R1072-R1084.
12. Egeblad, M., E.S. Nakasone, and Z. Werb, *Tumors as organs: complex tissues that interface with the entire organism.* Dev Cell, 2010. **18**(6): p. 884-901.
13. Gerhardt, H. and H. Semb, *Pericytes: gatekeepers in tumour cell metastasis?* J Mol Med (Berl), 2008. **86**(2): p. 135-44.
14. Lu, P., V.M. Weaver, and Z. Werb, *The extracellular matrix: a dynamic niche in cancer progression.* J Cell Biol, 2012. **196**(4): p. 395-406.
15. Grivennikov, S.I., F.R. Greten, and M. Karin, *Immunity, inflammation, and cancer.* Cell, 2010. **140**(6): p. 883-99.
16. Bremnes, R.M., et al., *The role of tumor stroma in cancer progression and prognosis: emphasis on carcinoma-associated fibroblasts and non-small cell lung cancer.* J Thorac Oncol, 2011. **6**(1): p. 209-17.
17. Korniluk, A., et al., *From inflammation to cancer.* Ir J Med Sci, 2017. **186**(1): p. 57-62.
18. Wroblewski, L.E., R.M. Peek, Jr., and K.T. Wilson, *Helicobacter pylori and gastric cancer: factors that modulate disease risk.* Clin Microbiol Rev, 2010. **23**(4): p. 713-39.
20. Coussens, L.M. and Z. Werb, *Inflammation and cancer.* Nature, 2002. **420**(6917): p. 860-7.

21. Dvorak, H.F., *Tumors: wounds that do not heal. Similarities between tumor stroma generation and wound healing.* N Engl J Med, 1986. **315**(26): p. 1650-9.

22. Shi, C. and E.G. Pamer, *Monocyte recruitment during infection and inflammation.* Nat Rev Immunol, 2011. **11**(11): p. 762-74.

23. Hao, N.B., et al., *Macrophages in tumor microenvironments and the progression of tumors.* Clin Dev Immunol, 2012. **2012**: p. 948098.

24. Wang, N., H. Liang, and K. Zen, *Molecular mechanisms that influence the macrophage m1-m2 polarization balance.* Front Immunol, 2014. **5**: p. 614.

25. Szebeni, G.J., et al., *Inflammation and Cancer: Extra- and Intracellular Determinants of Tumor-Associated Macrophages as Tumor Promoters.* Mediators Inflamm, 2017. **2017**: p. 9294018.

26. Yaal-Hahoshen, N., et al., *The chemokine CCL5 as a potential prognostic factor predicting disease progression in stage II breast cancer patients.* Clin Cancer Res, 2006. **12**(15): p. 4474-80.

27. Balkwill, F., *Cancer and the chemokine network.* Nat Rev Cancer, 2004. **4**(7): p. 540-50.

28. Lin, S., et al., *Chemokine C-C motif receptor 5 and C-C motif ligand 5 promote cancer cell migration under hypoxia.* Cancer Sci, 2012. **103**(5): p. 904-12.

29. Aldinucci, D. and A. Colombatti, *The inflammatory chemokine CCL5 and cancer progression.* Mediators Inflamm, 2014. **2014**: p. 292376.

30. Lv, D., et al., *CCL5 as a potential immunotherapeutic target in triple-negative breast cancer.* Cell Mol Immunol, 2013. **10**(4): p. 303-10.

31. Robinson, S.C., et al., *A chemokine receptor antagonist inhibits experimental breast tumor growth.* Cancer Res, 2003. **63**(23): p. 8360-5.

32. Suffee, N., et al., *Angiogenic properties of the chemokine RANTES/CCL5.* Biochem Soc Trans, 2011. **39**(6): p. 1649-53.

33. Khalid, A., et al., *Recent Advances in Discovering the Role of CCL5 in Metastatic Breast Cancer.* Mini Rev Med Chem, 2015. **15**(13): p. 1063-72.

34. Casola, A., et al., *Multiple cis regulatory elements control RANTES promoter activity in alveolar epithelial cells infected with respiratory syncytial virus.* J Virol, 2001. **75**(14): p. 6428-39.

35. Werner, T., et al., *Computer modeling of promoter organization as a tool to study transcriptional coregulation.* FASEB J, 2003. **17**(10): p. 1228-37.

36. Pritts, E.A., et al., *Peroxisome proliferator-activated receptor-gamma ligand inhibition of RANTES production by human endometriotic stromal cells is mediated through an upstream promoter element.* Fertil Steril, 2003. **80**(2): p. 415-20.

37. Schall, T.J., et al., *A human T cell-specific molecule is a member of a new gene family.* J Immunol, 1988. **141**(3): p. 1018-25.

38. Krensky, A.M. and Y.T. Ahn, *Mechanisms of disease: regulation of RANTES (CCL5) in renal disease.* Nat Clin Pract Nephrol, 2007. **3**(3): p. 164-70.

39. Kim, D.S., et al., *Fbw7gamma-mediated degradation of KLF13 prevents RANTES expression in resting human but not murine T lymphocytes.* Blood, 2012. **120**(8): p. 1658-67.

40. Raffetseder, U., et al., *Differential regulation of chemokine CCL5 expression in monocytes/macrophages and renal cells by Y-box protein-1.* Kidney Int, 2009. **75**(2): p. 185-96.

41. Rinkenbaugh, A.L. and A.S. Baldwin, *The NF-kappaB Pathway and Cancer Stem Cells.* Cells, 2016. **5**(2).

42. Yang, J., et al., *Unphosphorylated STAT3 accumulates in response to IL-6 and activates transcription by binding to NFkappaB.* Genes Dev, 2007. **21**(11): p. 1396-408.

43. Moore, M.J., *From birth to death: the complex lives of eukaryotic mRNAs.* Science, 2005. **309**(5740): p. 1514-8.

44. Wu, X. and G. Brewer, *The regulation of mRNA stability in mammalian cells: 2.0.* Gene, 2012. **500**(1): p. 10-21.

45. Decker, C.J. and R. Parker, *P-bodies and stress granules: possible roles in the control of translation and mRNA degradation.* Cold Spring Harb Perspect Biol, 2012. **4**(9): p. a012286.

46. Simone, L.E. and J.D. Keene, *Mechanisms coordinating ELAV/Hu mRNA regulons.* Curr Opin Genet Dev, 2013. **23**(1): p. 35-43.

47. Hinman, M.N. and H. Lou, *Diverse molecular functions of Hu proteins.* Cell Mol Life Sci, 2008. **65**(20): p. 3168-81.

48. Dalmau, J., et al., *The expression of the Hu (paraneoplastic encephalomyelitis/sensory neuronopathy) antigen in human normal and tumor tissues.* Am J Pathol, 1992. **141**(4): p. 881-6.

49. Ma, W.J., et al., *Cloning and characterization of HuR, a ubiquitously expressed Elav-like protein.* J Biol Chem, 1996. **271**(14): p. 8144-51.

50. Yates, B., et al., *Genenames.org: the HGNC and VGNC resources in 2017.* Nucleic Acids Res, 2017. **45**(D1): p. D619-D625.

51. Brennan, C.M. and J.A. Steitz, *HuR and mRNA stability.* Cell Mol Life Sci, 2001. **58**(2): p. 266-77.

52. Bakheet, T., B.R. Williams, and K.S. Khabar, *ARED 3.0: the large and diverse AU-rich transcriptome.* Nucleic Acids Res, 2006. **34**(Database issue): p. D111-4.

53. Khabar, K.S., *Hallmarks of cancer and AU-rich elements.* Wiley Interdiscip Rev RNA, 2017. **8**(1).

54. Abdelmohsen, K. and M. Gorospe, *Posttranscriptional regulation of cancer traits by HuR.* Wiley Interdiscip Rev RNA, 2010. **1**(2): p. 214-29.

55. Meng, Z., et al., *The ELAV RNA-stability factor HuR binds the 5'-untranslated region of the human IGF-IR transcript and differentially represses cap-dependent and IRES-mediated translation.* Nucleic Acids Res, 2005. **33**(9): p. 2962-79.

56. Mukherjee, J., et al., *PKM2 uses control of HuR localization to regulate p27 and cell cycle progression in human glioblastoma cells.* Int J Cancer, 2016. **139**(1): p. 99-111.

57. Fries, B., et al., *Analysis of nucleocytoplasmic trafficking of the HuR ligand APRIL and its influence on CD83 expression.* J Biol Chem, 2007. **282**(7): p. 4504-15.

58. Srikantan, S., K. Tominaga, and M. Gorospe, *Functional interplay between RNA-binding protein HuR and microRNAs.* Curr Protein Pept Sci, 2012. **13**(4): p. 372-9.

59. Kim, H.H., et al., *HuR recruits let-7/RISC to repress c-Myc expression.* Genes Dev, 2009. **23**(15): p. 1743-8.

60. Chang, N., et al., *HuR uses AUF1 as a cofactor to promote p16INK4 mRNA decay.* Mol Cell Biol, 2010. **30**(15): p. 3875-86.

61. Poria, D.K., et al., *RNA-binding protein HuR sequesters microRNA-21 to prevent translation repression of proinflammatory tumor suppressor gene programmed cell death 4.* Oncogene, 2016. **35**(13): p. 1703-15.

62. Izquierdo, J.M., *Hu antigen R (HuR) functions as an alternative pre-mRNA splicing regulator of Fas apoptosis-promoting receptor on exon definition.* J Biol Chem, 2008. **283**(27): p. 19077-84.

63. Dalmau, J., et al., *Detection of the anti-Hu antibody in the serum of patients with small cell lung cancer--a quantitative western blot analysis.* Ann Neurol, 1990. **27**(5): p. 544-52.

64. Zucal, C., et al., *Targeting the multifaceted HuR protein, benefits and caveats.* Curr Drug Targets, 2015. **16**(5): p. 499-515.

65. Kotta-Loizou, I., C. Giaginis, and S. Theocharis, *Clinical significance of HuR expression in human malignancy.* Med Oncol, 2014. **31**(9): p. 161.

66. Lopez de Silanes, I., A. Lal, and M. Gorospe, *HuR: post-transcriptional paths to malignancy.* RNA Biol, 2005. **2**(1): p. 11-3.

67. Kotta-Loizou, I., et al., *Current Evidence and Future Perspectives on HuR and Breast Cancer Development, Prognosis, and Treatment.* Neoplasia, 2016. **18**(11): p. 674-688.

68. Galban, S., et al., *RNA-binding proteins HuR and PTB promote the translation of hypoxia-inducible factor 1alpha.* Mol Cell Biol, 2008. **28**(1): p. 93-107.

69. Gubin, M.M., et al., *Overexpression of the RNA binding protein HuR impairs tumor growth in triple negative breast cancer associated with deficient angiogenesis.* Cell Cycle, 2010. **9**(16): p. 3337-46.

70. Mazan-Mamczarz, K., et al., *Post-transcriptional gene regulation by HuR promotes a more tumorigenic phenotype.* Oncogene, 2008. **27**(47): p. 6151-63.

71. Govindaraju, S. and B.S. Lee, *Adaptive and maladaptive expression of the mRNA regulatory protein HuR.* World J Biol Chem, 2013. **4**(4): p. 111-8.

72. Wang, J., et al., *Multiple functions of the RNA-binding protein HuR in cancer progression, treatment responses and prognosis.* Int J Mol Sci, 2013. **14**(5): p. 10015-41.

73. Shao, L., Z. Guo, and D.A. Geller, *Transcriptional suppression of cytokine-induced iNOS gene expression by IL-13 through IRF-1/ISRE signaling.* Biochem Biophys Res Commun, 2007. **362**(3): p. 582-6.

74. Tanaka, N. and T. Taniguchi, *The interferon regulatory factors and oncogenesis.* Semin Cancer Biol, 2000. **10**(2): p. 73-81.

75. Tamura, T., et al., *The IRF family transcription factors in immunity and oncogenesis.* Annu Rev Immunol, 2008. **26**: p. 535-84.

76. Takaoka, A., T. Tamura, and T. Taniguchi, *Interferon regulatory factor family of transcription factors and regulation of oncogenesis.* Cancer Sci, 2008. **99**(3): p. 467-78.

77. Lin, R., et al., *Selective DNA binding and association with the CREB binding protein coactivator contribute to differential activation of alpha/beta interferon genes by interferon regulatory factors 3 and 7.* Mol Cell Biol, 2000. **20**(17): p. 6342-53.

78. Cammas, A., et al., *Destabilization of nucleophosmin mRNA by the HuR/KSRP complex is required for muscle fibre formation.* Nat Commun, 2014. **5**: p. 4190.

79. Yiakouvaki, A., et al., *Myeloid cell expression of the RNA-binding protein HuR protects mice from pathologic inflammation and colorectal carcinogenesis.* J Clin Invest, 2012. **122**(1): p. 48-61.

80. Fan, J., et al., *Chemokine transcripts as targets of the RNA-binding protein HuR in human airway epithelium.* J Immunol, 2011. **186**(4): p. 2482-94.

81. Katsanou, V., et al., *HuR as a negative posttranscriptional modulator in inflammation.* Mol Cell, 2005. **19**(6): p. 777-89.

82. Gruber, A.R., et al., *ARESite: a database for the comprehensive investigation of AU-rich elements.* Nucleic Acids Res, 2011. **39**(Database issue): p. D66-9.

83. Koga, T., et al., *Virus-inducible expression of a host chemokine gene relies on replication-linked mRNA stabilization.* Proc Natl Acad Sci U S A, 1999. **96**(10): p. 5680-5.

84. Pazdrak, K., et al., *MAPK activation is involved in posttranscriptional regulation of RSV-induced RANTES gene expression.* Am J Physiol Lung Cell Mol Physiol, 2002. **283**(2): p. L364-72.

85. Li, Q.Q. and C.T. Bever, *Mechanisms underlying the synergistic effect of Th1 cytokines on RANTES chemokine production by human glial cells.* Int J Mol Med, 2001. **7**(2): p. 187-95.

86. Wolf, A., et al., *Identification and functional characterization of novel phosphorylation sites in TAK1-binding protein (TAB) 1.* PLoS One, 2011. **6**(12): p. e29256.

87. Vlasova-St Louis, I. and P.R. Bohjanen, *Post-transcriptional regulation of cytokine signaling by AU-rich and GU-rich elements.* J Interferon Cytokine Res, 2014. **34**(4): p. 233-41.

88. Vlasova-St Louis, I. and P.R. Bohjanen, *Post-transcriptional regulation of cytokine and growth factor signaling in cancer.* Cytokine Growth Factor Rev, 2017. **33**: p. 83-93.

89. Kudo, T., et al., *Regulation of RANTES promoter activation in gastric epithelial cells infected with Helicobacter pylori.* Infect Immun, 2005. **73**(11): p. 7602-12.

90. Pritts, E.A., et al., *PPAR-gamma decreases endometrial stromal cell transcription and translation of RANTES in vitro.* J Clin Endocrinol Metab, 2002. **87**(4): p. 1841-4.

91. Pimenta, E.M., et al., *IRF5 is a novel regulator of CXCL13 expression in breast cancer that regulates CXCR5(+) B- and T-cell trafficking to tumor-conditioned media.* Immunol Cell Biol, 2015. **93**(5): p. 486-99.

92. Bi, X., et al., *Loss of interferon regulatory factor 5 (IRF5) expression in human ductal carcinoma correlates with disease stage and contributes to metastasis.* Breast Cancer Res, 2011. **13**(6): p. R111.

93. Garaud, S. and K. Willard-Gallo, *IRF5: a rheostat for tumor-infiltrating lymphocyte trafficking in breast cancer?* Immunol Cell Biol, 2015. **93**(5): p. 425-6.

94. Yarilina, A., et al., *TNF activates an IRF1-dependent autocrine loop leading to sustained expression of chemokines and STAT1-dependent type I interferon-response genes.* Nat Immunol, 2008. **9**(4): p. 378-87.

95. Bridge, A.J., et al., *Induction of an interferon response by RNAi vectors in mammalian cells.* Nat Genet, 2003. **34**(3): p. 263-4.

96. Parkes, E.E., et al., *Activation of STING-Dependent Innate Immune Signaling By S-Phase-Specific DNA Damage in Breast Cancer.* J Natl Cancer Inst, 2017. **109**(1).

97. Mehta, M., et al., *HuR silencing elicits oxidative stress and DNA damage and sensitizes human triple-negative breast cancer cells to radiotherapy.* Oncotarget, 2016. **7**(40): p. 64820-64835.

98. Xu, H., et al., *Up-regulation of the interferon-related genes in BRCA2 knockout epithelial cells.* J Pathol, 2014. **234**(3): p. 386-97.

99. Tymoszuk, P., et al., *In situ proliferation contributes to accumulation of tumor-associated macrophages in spontaneous mammary tumors.* Eur J Immunol, 2014. **44**(8): p. 2247-62.

100. Velasco-Velazquez, M., W. Xolalpa, and R.G. Pestell, *The potential to target CCL5/CCR5 in breast cancer.* Expert Opin Ther Targets, 2014. **18**(11): p. 1265-75.

101. Latorre, E., et al., *The Ribonucleic Complex HuR-MALAT1 Represses CD133 Expression and Suppresses Epithelial-Mesenchymal Transition in Breast Cancer.* Cancer Res, 2016. **76**(9): p. 2626-36.

102. Guttilla, I.K., et al., *Prolonged mammosphere culture of MCF-7 cells induces an EMT and repression of the estrogen receptor by microRNAs.* Breast Cancer Res Treat, 2012. **132**(1): p. 75-85.

103. Licata, L.A., et al., *The RNA-binding protein HuR regulates GATA3 mRNA stability in human breast cancer cell lines.* Breast Cancer Res Treat, 2010. **122**(1): p. 55-63.

104. Pryzbylkowski, P., O. Obajimi, and J.C. Keen, *Trichostatin A and 5 Aza-2' deoxycytidine decrease estrogen receptor mRNA stability in ER positive MCF7 cells through modulation of HuR.* Breast Cancer Res Treat, 2008. **111**(1): p. 15-25.

105. Yan, W., et al., *Increased invasion and tumorigenicity capacity of CD44+/CD24- breast cancer MCF7 cells in vitro and in nude mice.* Cancer Cell Int, 2013. **13**(1): p. 62.

106. Long, H., et al., *Autocrine CCL5 signaling promotes invasion and migration of CD133+ ovarian cancer stem-like cells via NF-kappaB-mediated MMP-9 upregulation.* Stem Cells, 2012. **30**(10): p. 2309-19.

107. Heinonen, M., et al., *Cytoplasmic HuR expression is a prognostic factor in invasive ductal breast carcinoma.* Cancer Res, 2005. **65**(6): p. 2157-61.

108. Denkert, C., et al., *Expression of the ELAV-like protein HuR is associated with higher tumor grade and increased cyclooxygenase-2 expression in human breast carcinoma.* Clin Cancer Res, 2004. **10**(16): p. 5580-6.

7 Appendix

7.1 Buffers

7.1.1 Buffer and solutions for cell culture

Erythrocyte lysis buffer

NH_4Cl	155 mM
$KHCO_3$	10 mM
EDTA	0.1 mM

Trypsin EDTA

Trypsin	0.5 mg/mL
EDTA	0.22 mg/mL

Leukocyte running buffer

EDTA	2 mM
BSA	0.5% (w/v)
in PBS	

Leukocyte washing buffer

EDTA	2 mM
in PBS	

Cell freezing medium

DMSO	10% (v/v)
in FCS	

7.1.2 Buffer and solutions for immunohistochemistry

4% PFA (paraformaldehyde)

paraformaldehyde	4% (v/v)
in PBS	

ICC washing buffer

BSA	0.2% (w/v)
in PBS	

10x TBST

NaCl	300 mM
Tris	50 mM
→ pH 7.6	

Antibody diluent

BSA	1% (m/v)
Sodium azide	0.015 M
in TBS	

Tween 20	1% (v/v)

ICC permeabilization buffer

Triton X-100	0.1% (v/v)
BSA	0.2% (w/v)
in PBS	

7.1.3 Solutions for luciferase reporter assay

***Firefly* luciferase substrate**

Tricine	20 mM
$MgCO_3$ x $Mg(OH)_2$ x $5H_2O$	2.67 mM
$MgSO_4$ x $7H_2O$	1.07 mM
EDTA	100 µM
DTT	33.3 mM
ATP	530 µM
Coenzym A	0.21 mg/mL
D-luciferin	470 mM

***Renilla* luciferase substrate**

NaCl	100 mM
Tris-HCl pH 7.5	25 mM
$CaCl_2$	1 mM
Coelentherazine	1 µM

7.1.4 Buffer for Western analysis

10x blotting buffer

Tris/ HCl	250 mM
Glycine	1.9 M
→ pH 8.3	

1x blotting buffer

10x blotting buffer	10% (v/v)
Methanol	20% (v/v)
Tris-HCl	125 mM

BSA blocking solution

BSA-	5% (w/v)
in TBS	

ECL solution A

Tris-HCl
Luminol
→ pH 8.6

ECL solution B

pHydroxy-Cumaric-acid	6.7 mM
in DMSO	

Protein lysis buffer

Tris-HCl pH 6.8	10 mM
Urea	6.65 mM
Glycine	10% (w/v)
SDS	1% (w/v)
→ pH 7.4	
Add freshly prior to use	
PIM	1x
DTT	1 mM

4x SDS-PAGE sample buffer

Tris-HCl	125 mM
SDS	2% (w/v)
Glycerine	50% (v/v)
DTT	1 mM
Bromophenol blue	0.002% (w/v)
→ pH 6.9	

10x TBS

Tris-HCl	500 mM
NaCl	1.5 M
→ pH 7.4	

SDS running buffer

Tris-HCl	25 mM
Glycin	192 mM
SDS	700 µM
→ pH 8.3	

4 x upper Tris buffer

Tris-HCl	0.5 M
→ pH 6.8	

4 x lower Tris buffer

Tris-HCl	1.5 M
→ pH 8.8	

Cytosol lysis buffer

HEPES	10 mM
KCl	10 mM
EDTA	0.1 mM
EGTA	0.1 mM
Add freshly prior to use	
PIM	1x
DTT	1 mM
PMSF	0.5 mM

1x TBST

TBS	1x
Tween®20	0.05% (v/v)

SDS-polyacrylamide gels

	separating gel (12%)	**stacking gel (4%)**
40% Acrylamide/Bis-acrylamide (37.5%/1.0% w/v)	3 mL	300 µL
4 x lower Tris buffer	3 mL	
4 x upper Tris buffer		750 µL
H_2O distilled	4.4 mL	1.95 mL
10% SDS	100 µL	30 µL
TEMED	10 µL	2.5 µL
10% (w/v) ammonium persulfate	100 µL	25 µL

7.1.5 Buffer for ChIP assay

L1 buffer

HEPES/KOH pH 7.9	10 mM
KCl	85 mM
EDTA	1 mM
Add freshly prior to use	
PIM	1x
PMSF	1 mM

L2 buffer

SDS	1% (w/v)
Tris-HCl pH 7.4	50 mM
Empigen BB	0.5%
EDTA	10 mM
Add freshly prior to use	
PIM	1x
PMSF	1 mM

7.2 Thermal cycling programs for PCRs

Table 12: Program for semiquantitative real-time PCRs (qPCRs)

Cycles	Procedure	Temperature	Time
1x	denaturation and enzyme activation	95°C	3 min
40x	denaturation	95°C	15 s
	annealing	60°C	30 s
	elongation	72°C	30 s
1x	denaturation	95°C	30 s
1x	renaturation	72°C	30 s
80x (+0.5°C per cycle)	melting curve	60-95°C	5 s

Table 13: Program for standard cloning PCRs

Cycles	Procedure	Temperature	Time
1x	denaturation	94°C	2 min
35x	denaturation	94°C	45 s
	annealing	T_M - 5°C	30 s
	elongation	72°C	45 s
1x	final elongation	72°C	10 min

Table 14: Program for In-Fusion cloning PCRs

Cycles	Procedure	Temperature	Time
1x	denaturation	94°C	2 min
5x	denaturation	94°C	45 s
	annealing	45°C	30 s
	elongation	72°C	45 s
30x	denaturation	94°C	45 s
	annealing	T_M - 5°C	30 s
	elongation	72°C	45 s
1x	final elongation	72°C	10 min

8 Publications

M. M. Bajer, M. M. Kunze, J. S. Blees, H. R. Bokesch, H. Chen, **T. F. Brauss**, Z. Dong, K. R. Gustafson, R. M. Biondi, C. J. Henrich, J. B. McMahon, N. H. Colburn, T. Schmid, and B. Brüne, 'Characterization of Pomiferin Triacetate as a Novel mTOR and Translation Inhibitor', Biochem Pharmacol, 88 (2014), 313-21.

D. Rübsamen, M. M. Kunze, V. Buderus, **T. F. Brauss**, M. M. Bajer, B. Brüne, and T. Schmid, 'Inflammatory Conditions Induce IRES-Dependent Translation of Cyp24a1', PLoS One, 9 (2014), e85314.

A. Doller, A. Badawi, T. Schmid, **T. Brauss**, T. Pleli, D. M. zu Heringdorf, A. Piiper, J. Pfeilschifter, and W. Eberhardt, 'The Cytoskeletal Inhibitors Latrunculin a and Blebbistatin Exert Antitumorigenic Properties in Human Hepatocellular Carcinoma Cells by Interfering with Intracellular HuR Trafficking', Exp Cell Res, 330 (2015), 66-80.

N. Steinmeyer, A. Doller, A. Biyanee, **T. Brauss**, T. Schmid, J. Pfeilschifter, and W. Eberhardt, 'Lymphotoxin Alpha, a Novel Target of Posttranscriptional Gene Regulation by HuR in HepG2 Cells', FEBS Lett, 589 (2015), 1943-50.

M. M. Kunze, F. Benz, **T. F. Brauss**, S. Lampe, J. E. Weigand, J. Braun, F. M. Richter, I. Wittig, B. Brüne, and T. Schmid, 'sST2 Translation Is Regulated by FGF2 Via an hnRNP A1-Mediated IRES-Dependent Mechanism', Biochim Biophys Acta, 1859 (2016), 848-59.

T. F. Brauss, S. Winslow, S. Lampe, A. Scholz, A. Weigert, N. Dehne, K. von Stedingk, T. Schmid, and B. Brüne, 'The RNA-Binding Protein HuR Inhibits Expression of CCL5 and Limits Recruitment of Macrophages into Tumors', Mol Carcinog, 56 (2017), 2620-29.

S. Lampe, M. Kunze, A. Scholz, **T. F. Brauss**, S. Winslow, S. Simm, M. Keller, J. Heidler, I. Wittig, B. Brüne, and T. Schmid, 'Identification of the TXNIP IRES and Characterization of the Impact of Regulatory IRES Trans-Acting Factors', Biochim Biophys Acta Gene Regul Mech, 1861 (2018), 147-57.

S. Winslow, A. Scholz, P. Rappl, **T. F. Brauss**, C. Mertens, M. Jung, A. Weigert, B. Brüne, and T. Schmid, 'Macrophages Attenuate the Transcription of Cyp1a1 in Breast Tumor Cells and Enhance Their Proliferation', PLoS One, 14 (2019), e0209694.

10 Erklärung

Ich erkläre ehrenwörtlich, dass ich die am Fachbereich Biochemie, Chemie und Pharmazie der Johann Wolfgang Goethe-Universität in Frankfurt am Main zur Promotionsprüfung eingereichte Dissertation mit dem Titel

The role of HuR in the crosstalk
between tumor cells and macrophages

am Institut der Biochemie I / Pathobiochemie der Johann Wolfgang Goethe-Universität Frankfurt am Main unter Betreuung und Anleitung von Professor Dr. Bernhard Brüne mit Unterstützung durch Dr. Tobias Schmid ohne sonstige Hilfe selbst durchgeführt und bei der Abfassung der Arbeit keine anderen als die in der Dissertation angeführten Hilfsmittel benutzt habe.

Ich habe bisher an keiner in- oder ausländischen Universität ein Gesuch um Zulassung zur Promotion eingereicht. Die vorliegende Arbeit wurde bisher nicht als Dissertation eingereicht.

Teile der vorliegenden Arbeit wurden in Molecular Carcinogenesis veröffentlicht:

T. F. Brauss, S. Winslow, S. Lampe, A. Scholz, A. Weigert, N. Dehne, K. von Stedingk, T. Schmid, and B. Brüne, 'The RNA-Binding Protein HuR Inhibits Expression of CCL5 and Limits Recruitment of Macrophages into Tumors', Mol Carcinog, 56 (2017), 2620-29.

Frankfurt am Main, den

11 Danksagung

Ich möchte allen Personen danken, die durch fachliche Expertise und/oder moralische Unterstützung zum Entstehungsprozess dieser Arbeit beigetragen haben. Insbesondere gilt mein Dank:

Prof. Bernhard Brüne für den wissenschaftlichen Input und für sein großzügiges Entgegenkommen bei der Erstellung dieser Arbeit.

Prof. Dieter Steinhilber für seine Unterstützung, insbesondere für die spontane Bereitschaft, meine Arbeit seitens des Fachbereiches 14 zu betreuen.

Dr. Tobias Schmid für seinen beispiellosen Einsatz als PI und seine Leidenschaft als wissenschaftlicher Mentor.

Dr. Nathalie Dehne und Dr. Andreas Weigert, die stets ein offenes Ohr hatten bei Fragen bezüglich ChIP und FACS für ihre Hilfsbereitschaft sowie Dr. Kristoffer von Stedingk (Lund University) für die Unterstützung bei den in silico Analysen.

Michael, Sebastian, Anica und Sofia für buchstäblich jeden einzelnen Tag auf der Arbeit (und darüber hinaus). Ich hätte es nicht besser treffen können als mit euch, es war eine fantastische Zeit!

Dem gesamten Biochemie I Institut für die schöne Arbeitsatmosphäre, insbesondere Fabienne, Marina, Peter, Marcela und Tatjana für die oft nötige Auflockerung an langen Arbeitstagen.

An dieser Stelle muss ich untypischerweise eine Person ein zweites Mal erwähnen, da deren Einsatz für das Gelingen dieser Arbeit weit über das oben erwähnte hinausging. Danke Toby für deine unerschütterliche Zuversicht, deine stoische Gelassenheit, deine Sturheit und deine bedingungslose Loyalität. Ich weiß, was ich dir verdanke.

Zu guter Letzt möchte ich meiner Familie, meinen Freunden und Bandkollegen danken für ihre Unterstützung sowie die Geduld und das Verständnis, wenn sich mal wieder wegen mir Verabredungen und Albumreleasetermine nach hinten verschoben haben.

Danke euch allen!